Journal of Peptide Science
J. Peptide Sci. **6**: 57–83 (2000)

CD, ^{1}H NMR and Molecular Modeling Studies of the Interaction of Ca^{2+} with Substance P and Ala^7-Substance P in a Non-polar Solvent

XIAO-FEI QI, BORIS S. ZHOROV and VETTAI S. ANANTHANARAYANAN*

Department of Biochemistry, McMaster University, Hamilton, Ontario, Canada

Received 9 February 1999
Accepted 17 August 1999

Abstract: The biologically relevant conformation of substance P is likely to be dictated by the lipid milieu wherein the hormone would interact with its receptor. Assuming that specific constraints to the hormone structure may be imparted by its interaction with Ca^{2+} ions in the low dielectric lipid medium, the interaction of substance P and its inactive analog, Ala^7-substance P, has been characterized in a lipid-mimetic solvent. Circular dichroism (CD) and NMR spectral methods were employed to study the conformation of the free and Ca^{2+}-bound forms of the peptides and the conformational changes that occur on Ca^{2+} binding. The results show that both peptides assume a helical structure in the non-polar solvent used, a mixture of acetonitrile and trifluoroethanol. The *N*-terminal region is, however, less ordered in the analog peptide compared with the native hormone. Ca^{2+} addition causes significant conformational changes in both the peptides. However, while substance P binds two Ca^{2+} ions in a cooperative manner, Ala^7-substance P binds only one Ca^{2+} ion with a relatively weaker affinity. Computations of the minimum-energy conformations of the free and Ca^2-bound peptides were performed using *inter*proton distances derived from nuclear Overhauser enhancement spectra of the two peptides, as well as the information provided by changes in proton chemical shifts caused by Ca^{2+} addition. Taken together, the results of this study suggest that differences in the interaction of substance P and Ala^7-substance P with Ca^{2+} in the non-polar milieu, which in turn leads to differences in their Ca^{2+}-bound conformations, may be the basis for the differences in their biological potencies. Copyright © 2000 European Peptide Society and John Wiley & Sons, Ltd.

Keywords: bioactive structure; hormone–calcium interaction; molecular modeling; nuclear magnetic resonance; substance P

INTRODUCTION

The tachykinins are an important family of neuropeptides that are implicated in pain transmission, inflammation, smooth muscle contraction, hypotension and salivation [1,2]. Substance P (SP), an undecapeptide (sequence: Arg^1-Pro^2-Lys^3-Pro^4-Gln^5-Gln^6-Phe^7-Phe^8-Gly^9-Leu^{10}-Met^{11}-NH_2), is the most studied of the tachykinin peptides and is widely distributed in both the central and peripheral nervous systems. All tachykinin peptides contain the *C*-terminal sequence: Phe-Xxx-Gly-Leu-Met. This segment of tachykinins is regarded as the 'message' [3] region responsible for the biological activities of the hormone [4,5], while the *N*-terminal segment

Abbreviations: SP, substance P; Ala^7-SP, substance P with alanine in position 7; TFE, trifluoroethanol; TFE-d_2, 2,2,2-trifluoroethyl-1,1-d_2 alcohol; ACN, acetonitrile; ACN-TFE, 80:20 (v:v) acetonitrile and TFE; CD, circular dichroism; NMR, nuclear magnetic resonance; uv, ultraviolet; TOCSY, total correlation spectroscopy; NOESY, nuclear Overhauser spectroscopy; ROESY, rotating frame cross-relaxation spectroscopy; MCM, Monte Carlo with energy minimization; MEC, minimum-energy conformation; SRMCM, stochastically restrainable Monte Carlo minimization.

* Correspondence to: Department of Biochemistry, McMaster University, 1200 Main Street West, Hamilton, Ontario, Canada L8N 3Z5. E-mail: ananth@mcmaster.ca

CCC 1075–2617/2000/020057-27$17.50

(residues 1–6 in SP) is considered to be the 'address' [3] region, possessing binding affinity to the receptor. The biological effects elicited by SP are mediated through the activation of NK-1, one of three major neurokinin receptor subtypes. The transmembrane topology of the SP receptor, as inferred from its amino acid sequence [6], shows the seven-helix bundle arrangement seen in many other hormone and drug receptors.

Understanding the relationship between the structure and biological activity would assist in developing therapeutically valuable SP analogs [7]. A great deal of effort has, therefore, been put into the detailed structural analysis of SP. The hormone exists as an ensemble of flexible structures in water [8–13], although there is some evidence that some degree of hydrogen-bonded ordered structure may also be present [13]. It has been suggested that the lipid milieu in which most peptide hormones would interact with membrane-bound receptors may impose specific constraints on hormone structure [3,14,15], so that the structure determined in lipid bilayers or micelles is generally regarded as a closer approximation to the bioactive conformation of SP than the structure prevailing in water. With this in mind, several researchers have determined the structure of SP in solvents that are regarded as lipid-mimetics [16], such as methanol [8–12] and trifluoroethanol (TFE) [8,11,17], as well as in lipid micelles and bilayers [8,11,18–25]. While the results of these studies differ in specific details, they show that, in general, SP is capable of adopting a helical structure involving, in particularly, residues 7–11 in the *C*-terminal.

In addition to the lipid milieu, a peptide hormone would encounter millimolar concentrations of Ca^{2+} in the extracellular compartment, especially near the relatively low dielectric lipid–water interface. We had suggested that under such conditions, Ca^{2+} may bind to the peptide hormone and impose additional structural constraints on the hormone beyond what is dictated by the lipid milieu [26]. It is relevant to note that extracellular Ca^{2+} is necessary for the action of SP [27]. One possible reason for this may be that the Ca^{2+}-bound conformation of SP in the lipid environment may be required for receptor activation. Based on this rationale, we have, in an earlier study [17], examined the interaction of SP and its *N*- and *C*-terminal peptide fragments with Ca^{2+} in a lipid-mimetic solvent (a mixture of 80:20 (v:v) acetonitrile (ACN) and TFE; we will refer to this mixture from now on as ACN-TFE). Circular dichroism (CD) and fluorescence spectral data showed stoichiometric interaction of SP and its *C*-terminal peptide (residues 7–11) with Ca^{2+}. Both of them translocated Ca^{2+} across lipid bilayers in synthetic liposomes, demonstrating binding of the ion inside the lipid. In contrast, the *N*-terminal peptide (residues 1–6) showed only a very weak affinity for Ca^{2+}. In the present study, we have sought to characterize the structures of free and Ca^{2+}-bound SP in the above solvent using CD, two-dimensional NMR and molecular modeling techniques. With the aim of seeking a correlation between biological potency and Ca^{2+}-bound conformation, we have also carried out a similar set of studies on an SP analog, Ala^7-SP, which is a very weak agonist analog of SP [28]. The results obtained show that while SP binds two Ca^{2+} ions in a biphasic manner with a moderate affinity, the weakly active Ala^7-SP binds only one Ca^{2+} with a relatively low affinity. The computed Ca^{2+}-bound conformations of SP and Ala^7-SP are substantially different. These data lend support to the suggestion that the Ca^{2+}-bound conformation of SP may be involved in receptor activation [26].

MATERIALS AND METHODS

Materials

Substance P (purity 99%) was purchased from Sigma (St. Louis, MO). SP and was used without further purification. Ala^7-SP was synthesized at the Biotechnology Service Centre, University of Toronto, and was purified by reversed-phase high-performance liquid chromatography (RP-HPLC) to over 95% (as determined by mass spectral analysis). ACN was bought from BDH Chemicals (Canada). TFE was obtained from Sigma and was distilled under vacuum before use. 2,2,2-Trifluoroethyl-l,1-d_2 alcohol (TFE-d_2) and acetonitrile-d_3 (ACN-d_3) were obtained from Isotec, Inc. (Miamisburg, OH). Calcium perchlorate [$Ca(ClO_4)_2 \cdot H_2O$] from VWR Scientific (Mississauga, Ontario) was lyophilized overnight under vacuum to remove water.

Methods

CD experiments. CD spectra were acquired on a Jasco J-600 spectropolarimeter using water-jacketed 1-cm quartz cell. The concentrations of SP and Ala^7-SP solutions were around 75 μM and 50 μM, respectively, and were determined from the extinction coefficient of the phenylalanyl residue (230 $M^{-1}\,cm^{-1}$ at 257.4 nm). The latter was obtained

from absorption measurements on an accurately weighed sample of lyophilized, dry SP in ACN-TFE. For Ca^{2+} titrations, aliquots of stock solutions of $Ca(ClO_4)_2$ in ACN-TFE solutions were added to the SP or Ala^7-SP solution inside the l cm cell with thorough mixing. CD spectra were recorded at ambient temperature (23 ± 2°C). The mean residue molar ellipticity [θ] was expressed in ° cm^2 $dmol^{-1}$. An average of 8–16 scans was obtained for each sample with appropriate baseline correction for the solvent.

NMR experiments. ^1H NMR experiments were performed on a Bruker DRX-500 spectrometer, operating at 500.13 MHz for proton resonance frequency. All experiments were performed at 27 ± 1°C. Chemical shifts were calibrated with reference to the TFE-d_2 proton signal at 3.88 ppm and solvent suppression was accomplished by using a 1.5 s pre-saturation pulse set at this frequency. The one-dimensional spectra were acquired with a spectral width of 5733.9 Hz to a digital resolution of 0.175 Hz. A total of 56 and 160 scans were acquired in the experiments on the free peptides and their Ca^{2+} complexes, respectively. The concentrations of SP and Ala^7-SP in ACN-d_3:TFE-d_2 (80:20, v:v) were typically between 3 and 5 mM. Metal ion titrations were done by adding aliquots of stock $Ca(ClO_4)_2$ solution (35–130 mM) in the above solvent mixture to a solution of SP and Ala^7-SP inside a 5 mm NMR tube. Proton chemical shifts and spectral line widths did not show any significant dependence on the concentrations of SP and Ala^7-SP in the range of 1–5 mM and 1–7 mM, respectively, pointing to absence of significant peptide aggregation. Lack of aggregation at 5 mM SP concentration has been noted by Woolley and Deber [19] who used CD as a check for SP aggregation.

Proton chemical shifts and sequential resonance assignments of SP were determined from TOCSY [29] and NOESY [30] data. The cross-peaks in the NOESY spectra of Ala^7-SP were relatively weak and limited in number compared with those in the ROESY [31] spectra of the peptide. The latter data were, therefore, used for the sequential resonance assignments for this peptide. All the two-dimensional data were acquired in the phase-sensitive mode and solvent suppression was accomplished using a 1.0 s pre-saturation pulse set at the frequency of TFE-d_2. The TOCSY spectra were acquired with a total spin-lock mixing time of 99 ms, using a MLEV-17 mixing sequence [32] with a 2.5 ms trim pulse. A total of 8–80 scans were acquired for the experiments of free peptide and relevant Ca^{2+} titrations, respectively. The time–domain matrix consisting of 2048×256 complex data points was acquired and then zero-filled to obtain the frequency domain matrix of 2048×1024 complex data points with a spectral width of 5000 Hz. A $\pi/2$ shifted sine-bell-squared window function was used in both dimensions. A digital resolution of 2.441 Hz was obtained.

From the NOESY and ROESY data of the peptides acquired at different mixing times, an optimal mixing time (τ_m) of 200–300 ms was chosen to obtain NOE and ROE cross-peaks with optimal signal-to-noise ratios. The number of scans acquired in the NOESY experiments on SP were 480, 520 and 560, respectively, for the Ca^{2+}-free peptide, 1:1 Ca^{2+}:peptide complex and 2:1 Ca^{2+}:peptide complex. A total of 160 and 240 scans were acquired, respectively, for the ROESY experiments on Ca^{2+}-free and Ca^{2+}-saturated Ala^7-SP. The NOESY and ROSEY data were processed similar to the TOCSY data. *Inter*proton distances were evaluated from the volume of integrals of NOE and ROE cross-peaks in the NOESY and ROESY spectra using the 1/(distance)^6 relationship [31] to measure the extent of transfer of magnetization between the spin systems during the NOE and ROE mixing times. These distances were calibrated against a reference distance of 1.85 Å between the β-CH_2 protons of the Phe^8 residue in SP and those of the Phe^7 residue in the case of the 1:1 and 1:1 Ca^{2+}:peptide complexes. In the case of Ala^7-SP, the β-CH_2 protons of the Phe^8 residue were used as the reference in the free as well as Ca^{2+}-saturated peptide experiments.

Molecular modeling. The ECEPP/2 force field [33] was used for calculations on the free and Ca^{2+}-bound forms SP and Ala^7-SP. The three basic groups in the peptides were considered in their neutral forms, assuming that their positive charges are neutralized by counter ions. Such a treatment of ionizable residues is standard in applications using the ECEPP/2 force field. All calculations were done in vacuum. The interactions between atoms were calculated with the cut-off distance of 8.5 Å; interactions between Ca^{2+} ions were calculated at all the distances. All torsion angles, coordinates of Ca^{2+} ions, and bond angles of the atoms in proline rings were varied in energy minimizations. Ca^{2+} was modeled as an oxygen atom with a double proton charge [34]. A dielectric constant of 2 was used in the calculations of the structures of the free peptides and the 1:1 Ca^{2+} complexes. In the calculations of 2:1 Ca^{2+}:SP complex, a distance-dependent dielectric constant was used in order to diminish strong repulsion of the

two cations that were not counterbalanced by anions.

The Monte Carlo with energy minimization (MCM) protocol of Li and Scheraga [35] was used for the search of optimal conformations as described elsewhere [34]. Energy calculations were carried out on the Indigo 2 extreme workstation (Silicon Graphics, CA) using the ZMM molecular modeling package [36]. Structures were visualized using Insight II software (BioSym Inc., CA). Two minimum-energy conformations (MECs) having the same backbone letter code [37] were considered to be similar if the difference in the analogous side-chain torsions were less than 10°. Non-similar MECs with the energies < 10 kcal mol^{-1} from the corresponding apparent global minimum were accumulated in files and sorted in the order of increasing energies.

*Inter*proton distances obtained from NOE data were taken into account as flat-bottom constraints [38] and were added to the conformational energy. Instead of applying all the NOE constraints simultaneously in the MCM search, which would yield MECs of unrealistic 'average' conformations, we used the stochastically restrainable Monte Carlo minimization (SRMCM) procedure, a component of the ZMM package [36], to treat the NOE constraints, as was recently done in analyzing the NOE data on oxytocin [39]. This procedure randomly 'activates' and 'inactivates' individual constraints during the MCM search and drives the trajectory to low-energy regions fitting as many NOEs as possible. If a given NOE is inconsistent with a current geometry, a random activation of the corresponding constraint would yield a high-energy MEC, which would have a low probability to be accepted into the trajectory. To ensure that a maximum number of NOEs be matched in the optimal MECs, we applied an energy benefit (E_{mc}) of -1 kcal mol^{-1} for each matched NOE. Thus, we biased conformations consistent with NMR data even if their energy was higher than the energy of the optimal MEC found without restrains. This bias may compensate partially for the simplified treatment of the environment and any approximations of energy terms in the ECEPP/2 force field.

RESULTS

CD spectral changes. The far-uv CD spectra of SP in ACN-TFE in the native and Ca^{2+}-bound forms have been reported earlier [17]. They were repeated in this study with a view to comparing the structures and Ca^{2+} interactions of SP and Ala^7-SP under identical conditions. The data are shown in Figure 1. The spectral features of SP (minima at 222 and 212 nm) are indicative of a β-turn (particularly the type III or 3_{10}-helix) or an α-helical structure [40]. This is consistent with earlier CD data of the hormone in a polar solvent, lipid micelles and bilayers [8–12,19,23]. In comparison, the CD spectrum of Ala^7-SP (Figure 1) indicates a relatively much weaker helical structure for this peptide, the magnitudes of the helical CD bands being less than half of those for SP. The overall shape of the CD spectrum of Ala^7-SP is however, suggestive of a helical structure admixed with the random coil form.

Addition of Ca^{2+} to SP resulted in a biphasic CD spectral change (Figure 1) as observed earlier [17] with saturation of Ca^{2+} binding occurring at about 2:1 Ca^{2+}:peptide molar ratio (Figure 1, inset). (The reason for the absence of CD changes in the early part of the cation titration (up to about 0.6 mole ratio of Ca^{2+} is unclear.) The 220 nm CD band in Ca^{2+}-saturated SP was positive in sign in contrast to its negative sign in the free peptide (Fig. l), suggesting a major difference in the conformations of these molecules. Addition of a three molar excess EDTA to the Ca^{2+}-saturated peptide caused a reversal of the CD spectrum back to that of free SP (data not shown). The rather unusual CD spectral pattern of Ca^{2+}-saturated SP is likely to arise from a secondary structure peculiar to the cation-bound peptide.

Titration of Ala^7-SP with Ca^{2+} caused CD changes (Figure 1) that were qualitatively similar to those obtained for SP, including the reversal of the sign of the 220 nm CD band. However, the magnitude of the net spectral change was much smaller than that observed in SP (Figure 1). The shallow binding curve with an apparent saturation of binding at an unrealistically high Ca^{2+}:peptide ratio of about 7 is possibly due to a weak affinity of the peptide for the cation. Extrapolation of the initial and final slopes of the binding isotherm indicated that saturation occurred at a Ca^{2+}:peptide ratio of 1 (Figure 1, inset). This was further verified by Ca^{2+} titration data in pure TFE, where SP showed a biphasic binding of two cations [17], while Ala^7-SP bound only one Ca^{2+} (Figure 1, top inset). These findings are compatible with the NMR data presented below. In view of the complex nature of the binding isotherms, the binding affinities of this complex and the cation complexes of SP have not been determined but are likely to lie in the range of 10^4 M (or M^2) based on the peptide concentrations needed to visualize the complexes. Monovalent (K^+ or Na^+) ions did not cause any significant CD changes even at high (100 molar excess) concentrations.

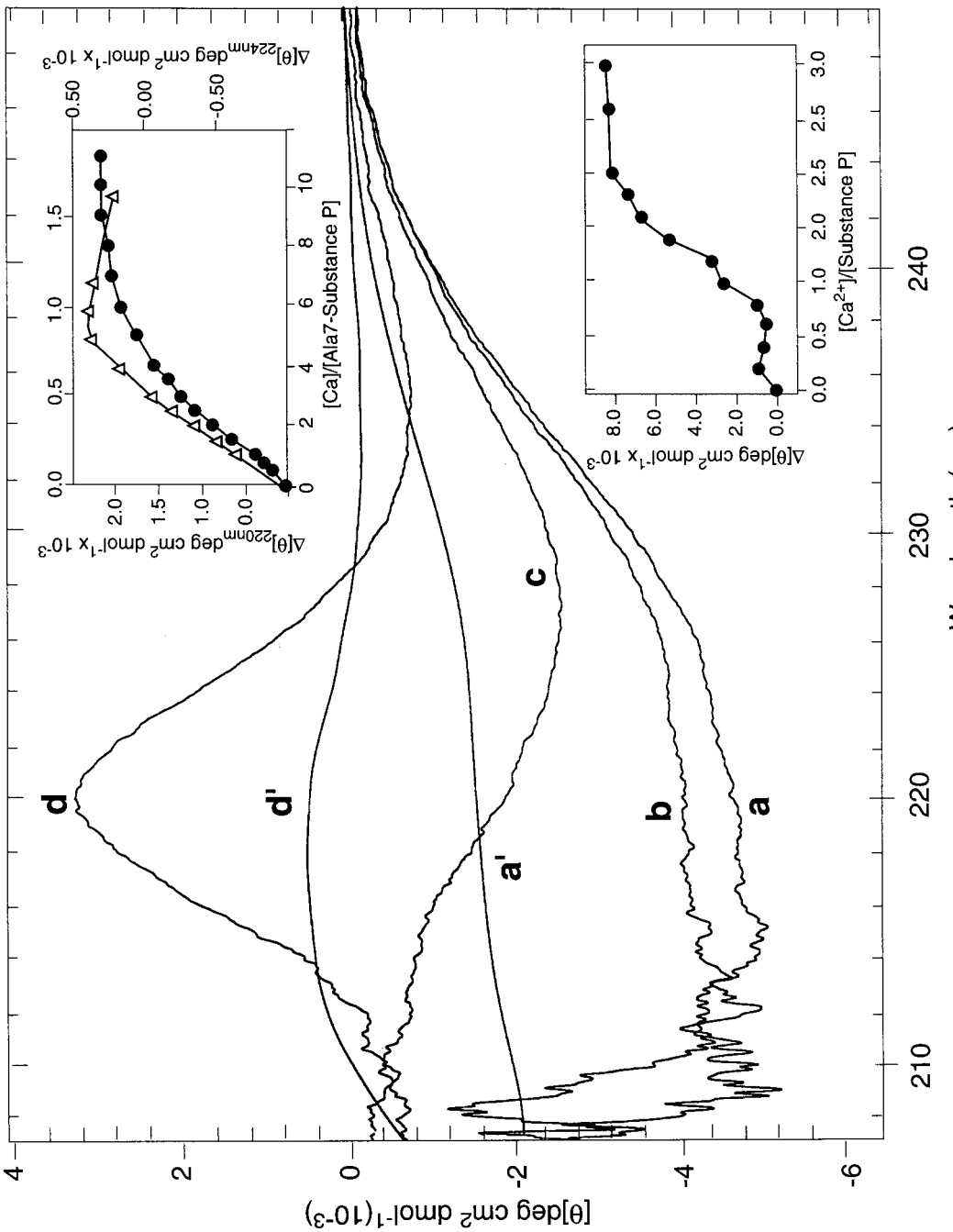

Figure 1 CD spectra of SP (70–76 μM) and Ala^7-SP (50–59 μM) at 22 ± 1° in 80:20 (v:v) ACN:TFE. (a) SP; (b) 0.5:1 Ca^{2+}:SP; (c) 1:1 Ca^{2+}:SP; (d) 2:1 Ca^{2+}:SP; (a′) Ala^7-SP; (d′) 6:1 Ca^{2+}:Ala^7-SP. Top inset: Ca^{2+} binding curves of Ala^7-SP obtained from changes in ellipticity at 224 nm for data in TFE (–△–; right ordinate) and in 80:20 (v:v) ACN:TFE (–●–; left ordinate). Bottom inset: Ca^{2+} binding curve of SP obtained from changes of ellipticity at 220 nm in 80:20 (v:v) ACN:TFE.

NMR data. Proton NMR data on SP, Ala^7-SP and their Ca^{2+} complexes were obtained in 80:20 (v:v) ACN-d_3:TFE-d_2. This solvent system was chosen instead of pure TFE-d_2 in light of the CD data that suggested enhanced amounts of the helical structure and larger magnitudes of structural changes on Ca^{2+} addition for these peptides in this mixed solvent (Figure 1 and Reference [17]). Chemical shifts assignments for SP and its Ca^{2+}-bound forms were accomplished in a straightforward manner by the combination of TOCSY and NOESY experiments using the technique of sequence-specific resonance assignments [31,41].

TOCSY spectra of SP, 0.5:1 Ca^{2+}:SP, 1:1 Ca^{2+}:SP and 2:1 Ca^{2+}:SP in the NH and aliphatic region are shown in Figure 2(a)–(c) to illustrate the *intra* residue cross-peaks generated among members of a coupled spin network. These data were used in the assignment of the chemical shifts of individual protons and were particularly helpful in following the movement of peaks during the Ca^{2+} titration and assigning resonances of protons with relatively large line widths. The chemical shifts of geminal protons, such as the αH protons of Gly^9 and βH protons of Phe^7, were well resolved in the aliphatic–aliphatic region with enhanced spectral resolution and sensitivity.

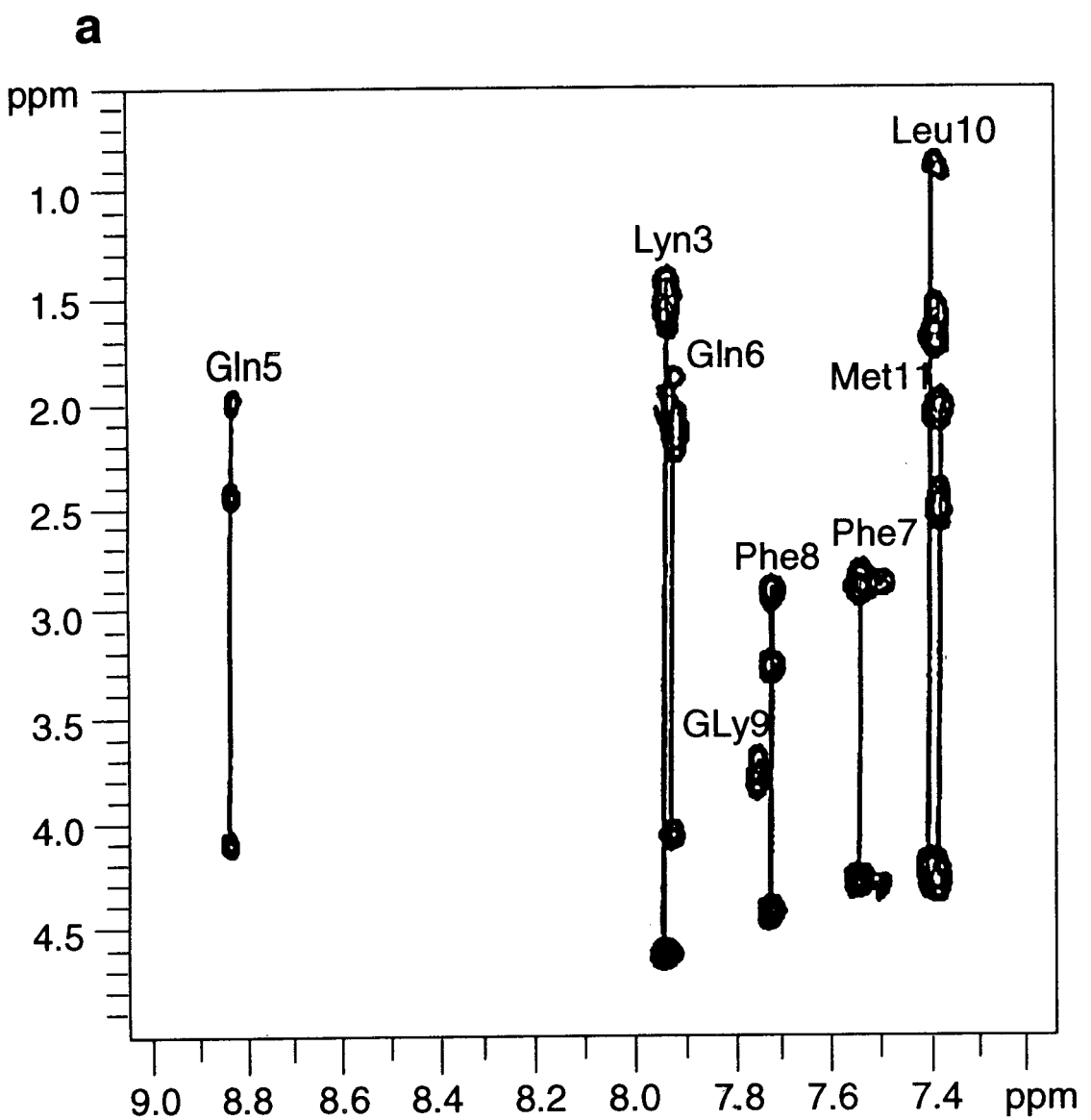

Figure 2 TOCSY spectra in 80:20 (v:v) ACN-d_3:TFE d_2 showing the amide–aliphatic regions of: (a) SP; (b)1:1 Ca^{2+}:SP; (c) 2:1 Ca^{2+}:SP.

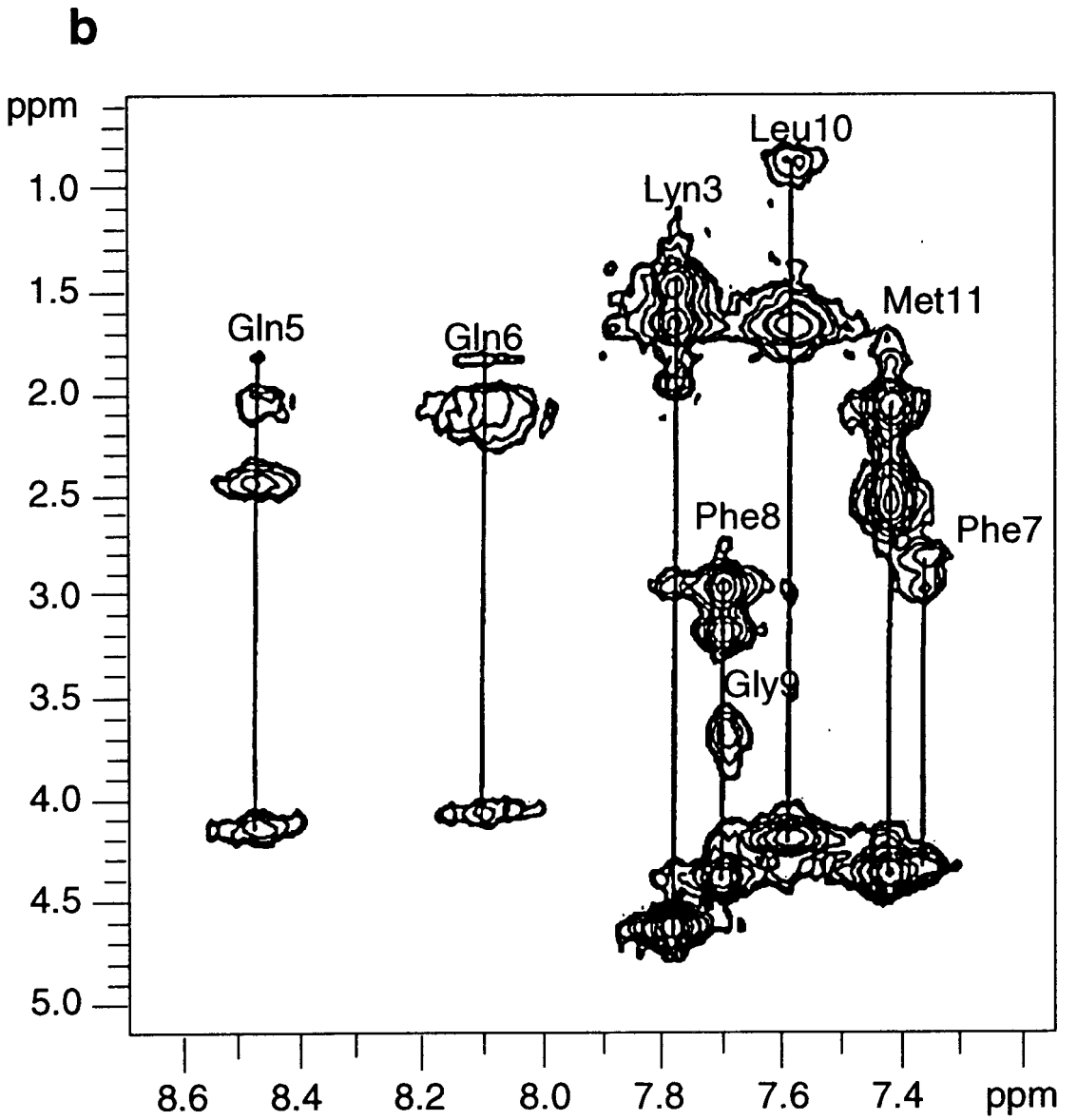

Figure 2 (*Continued*)

Since proline does not have an amide proton, the assignments of Pro^2 and Pro^4 spin systems were also carried out in the aliphatic region of the spectrum. The cross-peak between the amide and α protons of Arg^1 was not observable. After assigning the residue-specific spin systems, the sequential connectivities in the peptides were designated using the NOESY spectra. Some medium-range NOE connectivities were also used when the short-range NOE cross-peaks were severely overlapped or were not observable. The residue pairs Pro^2 and Pro^4, Gln^5 and Gln^6, Phe^7 and Phe^3 were well distinguished by their sequential NOE connectivities which, in turn, confirmed the chemical shift assignments for these residues made from TOCSY data. The assignments of some of the sequential NOE connectivities in SP and its 1:1, 2:1 Ca^{2+}:complexes are illustrated in the NOESY spectra (τ_m: 200 ms) shown in Figure 3(a)–(c). The proton chemical shift values for these molecules are listed in Table 1.

Chemical shift assignments for Ala^7-SP were accomplished using the chemical shift dispersions and connectivities in the TOCSY (Figure 4(a)) and ROESY (Figure 4(b)) spectra. Most of the assignments in Ala^7-SP were similar to those of the native hormone. However, unlike SP, Arg^1 was observed clearly in the

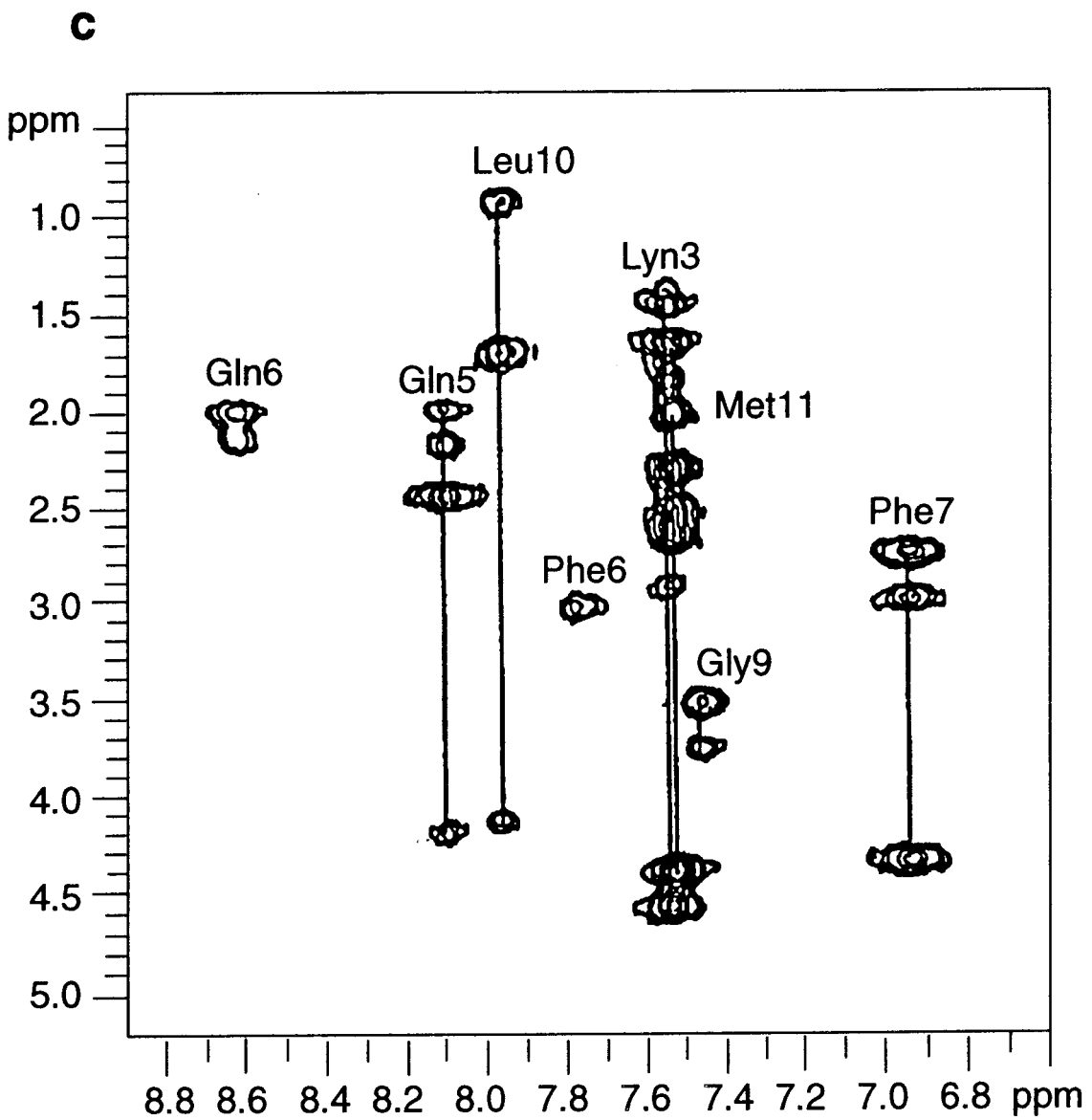

Figure 2 (*Continued*)

amide–aliphatic region of Ala^7-SP, while Ala^7 was well identified by its unique connection between the α and β protons. ROE signals of short and medium connectivities were found for Ala^7-SP enabling unambiguous chemical shift assignments for all the residues. Unlike SP, most residues in Ala^7-SP showed a small population of minor conformers (Figure 4(a)). That this did not arise from the chemical exchange caused by *cis* $\rightleftarrows$ *trans* isomerization of the peptide bonds involving Pro^2 and Pro^4 was inferred from the observation of two pairs of strong ROE cross-peaks between Arg^1 α and Pro^2 δ, Lys^3 α and Pro^4 δ protons (Figure 5). These cross-peaks can arise only from the *trans* conformation of the Arg^1-Pro^2 and Lys^3-Pro^4 peptide bonds. The exact origin of the minor bands is not clear. The very weak intensities of the minor cross-peaks in the ROESY spectra indicated that the population of the minor conformer, existing in equilibrium with the major conformer, was relatively very small. We have, therefore, concentrated our effort only on the major species. Complete assignment of proton chemical shifts for Ca^{2+}-saturated Ala^7-SP was hampered by the overwhelming line-broadening in the amide–aliphatic (Figure 4(c)) and amide–amide regions of the TOCSY spectra. Therefore, assignments had to be made

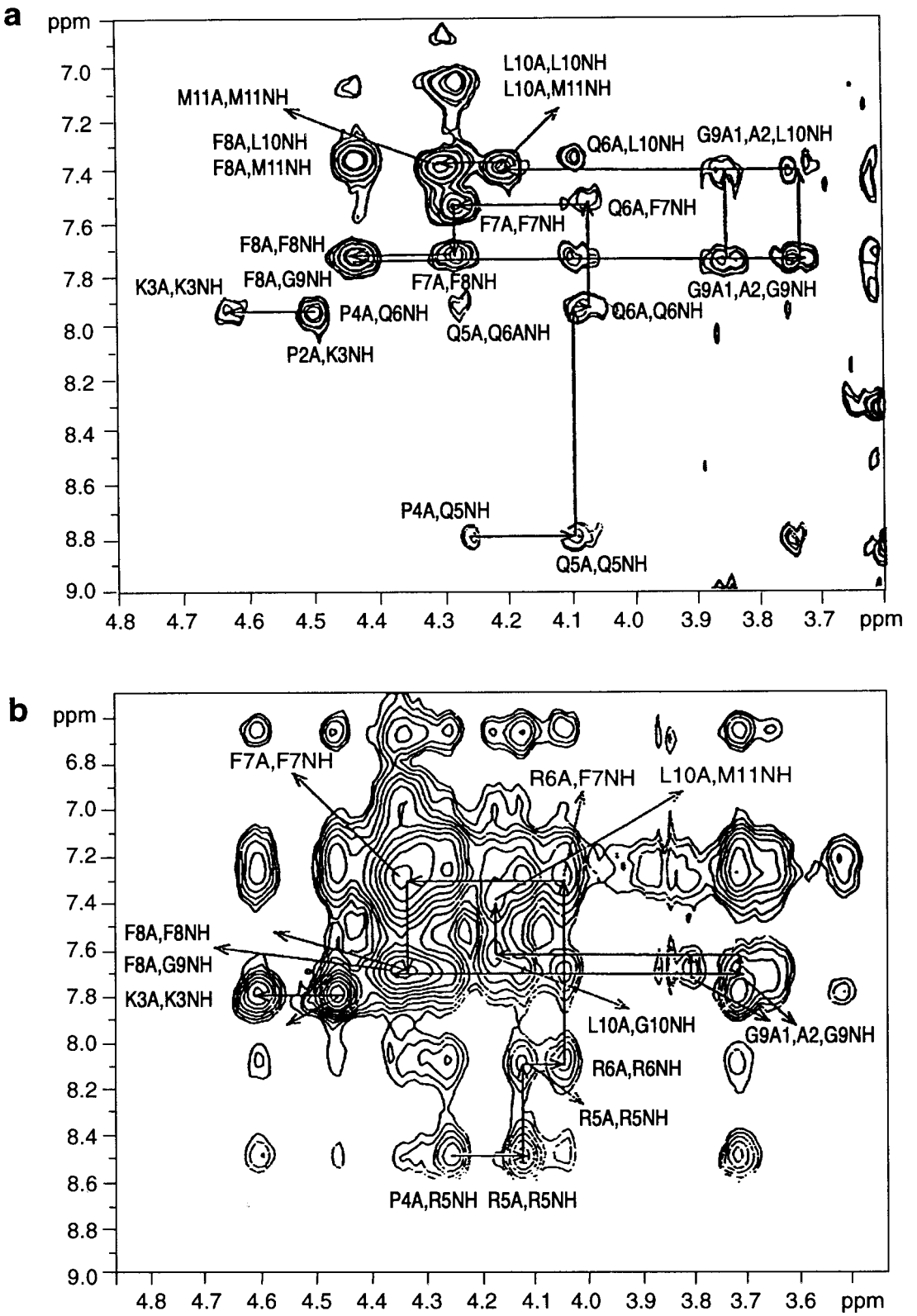

Figure 3 NOESY spectra in 80:20 (v:v) ACN-d_3:TFE d_2 in amide-α proton regions of: (a) SP; (b) 1:1 Ca^{2+}:SP; (c) 2:1 Ca^{2+}:SP.

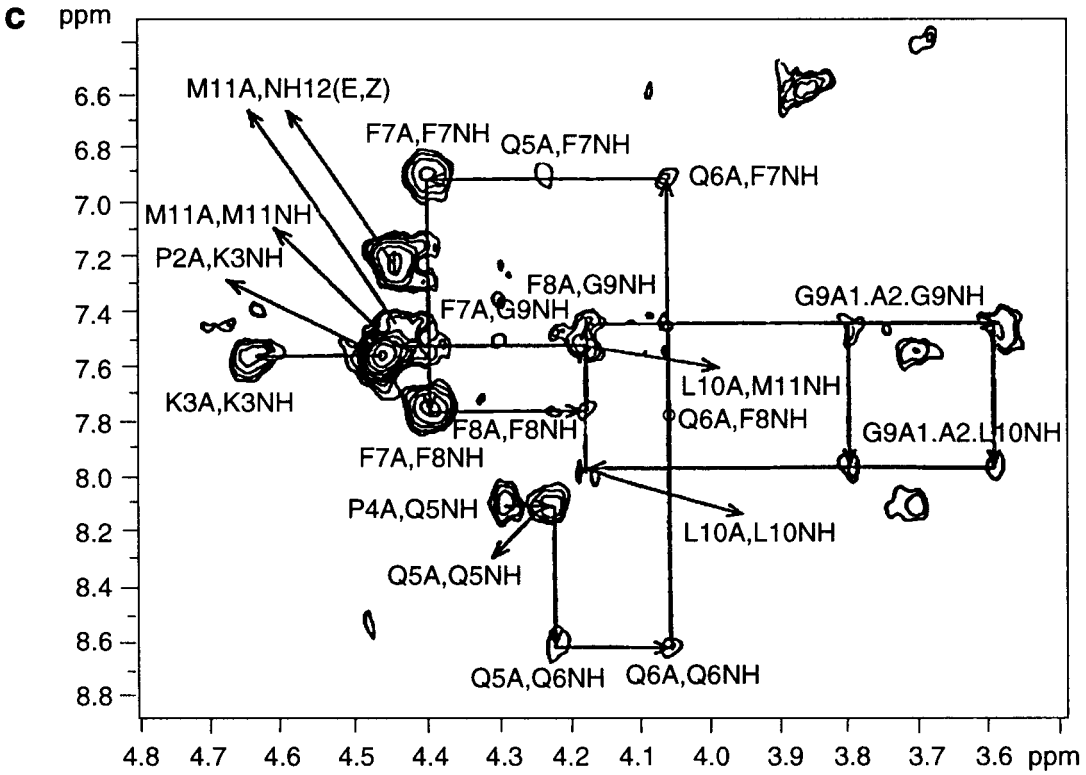

Figure 3 (*Continued*)

based on through-bond connectivities traced from the TOCSY spectra in the aliphatic region and from the changes in chemical shifts of residues during Ca^{2+} titration of Ala^7-SP. The latter were monitored using amide–aliphatic spin-coupling connectivities in the TOCSY spectra at different Ca^{2+}:peptide mole ratios. The *N*-terminal residues Arg^1, Pro^2, Lys^3 and Pro^4 as well as Gly^9 in the *C*-terminal showed strong spin coupled amide–aliphatic and aliphatic–aliphatic cross-peaks for the both major and minor species in the TOCSY spectra. Poor and weak ROE *intra*residual signals prevented their use in sequential chemical shift assignments. However, two pairs of strong ROE cross-peaks between Arg^1 α and Pro^2 δ, Lys^3 α and Pro^4 δ protons still existed indicating that, as in the Ca^{2+}-free form, *trans* peptide bonds prevail in both the major and minor conformers. Proton chemical shifts assignments for Ala^7-SP in the free and Ca^{2+}-saturated forms are listed in Table 2.

The magnitudes of proton chemical shifts (δ) in proteins and peptides are known to contain conformational information [42]. Changes in the chemical shift of a given proton in different solvents are attributable to changes in the peptide conformation in addition to those caused by solvation. In Figure 6, the δ values of the NH and αH protons of SP in ACN-TFE are compared, after subtraction of the δ values of the random coil values [31], with those of SP reported in earlier NMR studies in methanol [9,10], DMSO [9], dodecylphosphocholine (DPC) micelles [23,24] and SDS micelles [23]. It is seen from these comparisons that the amide proton chemical shifts for the residues between Gln^6 and Leu^{10} move upfield when SP is transferred from an aqueous solution to an apolar or lipid membrane environment, where these residues would adopt a folded structure [41]. The occurrence of the upfield shift (ranging from 0.15 to 0.60 ppm) for four or more contiguous residues without interruption would suggest a helical structure for that region [42]. By this criterion, residues Gln^6-Leu^{10} in SP may be inferred to adopt a helical structure in 80:20 (v:v) ACN:TFE mixture and in the lipid micelles. This would justify the use of the former solvent as a lipid mimetic.

Ca^{2+} titrations. To investigate the conformational changes that occur in SP and Ala^7-SP on binding Ca^{2+}, NMR data were collected at different Ca^{2+}:peptide molar ratios. Figure 7 shows the effect of

Ca^{2+} addition on the chemical shifts of amide protons (except for Arg^1) in SP and Ala^7-SP. With SP, the NMR-based Ca^{2+}-binding curves for the individual protons closely resembled the binding profile of the entire peptide observed by CD changes (Figure 1). Thus, most amide protons showed relatively much smaller changes in their chemical shifts until a Ca^{2+}:peptide ratio of ~ 0.8 was reached (Figure 7). Except for Phe^8 and Met^{11}, which displayed relatively much smaller changes, all the other amide protons underwent substantial changes in their chemical shifts and showed a saturation of cation binding at a ratio of 2:1 Ca^{2+}:SP (Figure 7). The largest changes were seen with Gln^5, Gln^6 and Phe^7 ($\Delta\delta > 0.6$ ppm). These observations, combined with the NOE data (see below), were fed into the molecular modeling computations to obtain the details of the peptide backbone changes that occur on Ca^{2+} binding to SP. Ca^{2+}-induced chemical shift changes in Ala^7-SP, shown in Figure 7, seem complicated, in that the

Table 1 Proton Chemical Shift (δ) Assignments for SP and its Ca^{2+} Complexes in 80:20 (v:v) ACN-d_3:TFE-d_2 at 300 K

Peptide/residue	NH	αH	βH	γH	Other
SP					
Arg^1	n	3.70	1.95, 1.91	1.68, 1.56	δCH_2: 3.08
Pro^2		4.50	2.19, 2.01	1.94, 1.89	δCH_2: 3.65, 3.54
Lys^3	7.93	4.62	1.96, 1.63	1.45	δCH_2: 1.54, εCH_2: 2.81
Pro^4		4.27	2.37, 2.13	2.03, 1.99	δCH_2: 3.76
Gln^5	8.81	4.10	2.04, 1.98	2.46, 2.42	δNH_2: 6.65, 6.05
Gln^6	7.91	4.06	2.06, 1.97	2.24, 2.17	δNH_2: 6.63,6.05
Phe^7	7.53	4.27	2.91, 2.84		2,6H: 7.05, 3, 5H:7.18
Phe^8	7.71	4.42	3.28, 2.91		2,6H: 7.25, 3, 5H: 7.33
Gly^9	7.74	3.85, 3.73			
Leu^{10}	7.37	4.21	1.58, 1.56	1.73	δCH_2: 0.93, 0.88
Met^{11}	7.36	4.30	2.08, 2.00	2.55, 2.45	NH_2: 6.83, 6.24
1:1 SP:Ca^{2+}					
Arg^1	n	3.73	1.72, 1.55	1.55	δCH_2: n
Pro^2		4.47	2.20, 2.02	1.95, 1.87	δCH_2: 3.67, 3.54
Lys^3	7.78	4.61	1.96	1.48	δCH_2: 1.65, εCH_2: 2.95
Pro^4		4.27	2.34, 2.10	2.01	δCH_2: 3.74
Gln^5	8.47	4.13	2.11, 1.98	2.45	δNH_2: 6.67,6.04
Gln^6	8.09	4.06	2.03, 1.97	2.23, 2.15	δNH_2: 6.68, 6.21
Phe^7	7.34	4.32	2.97, 2.82		2, 6H: 7.14, 3, 5H: 7.21
Phe^8	7.70	4.36	3.19, 2.96		2, 6H: 7.22, 3, 5H: 7.31
Gly^9	7.69	3.85, 3.69			
Leu^{10}	7.58	4.19	1.69, 1.62	1.75	δCH_2: 0.93, 0.88
Met^{11}	7.42	4.35	2.09, 2.04	2.59, 2.48	NH_2: 7.30, 6.97
1:2 SP:Ca^{2+}					
Arg^1	n	3.77	1.74, 1.56	1.62	δCH_2: 3.16
Pro^2		4.45	2.21, 2.04	1.95, 1.89	δCH_2: 3.68, 3.57
Lys^3	7.51	4.61	1.89, 1.67	1.48	δCH_2: 1.42, εCH_2: 2.98
Pro^4	8.08	4.31	2.28	2.02	δH_2: 3.71
Gln^5	8.62	4.22	2.21, 2.01	2.47	δNH_2: 6.67, 5.89
Gln^6	6.89	4.05	2.02	2.17	δNH_2: 6.61, 6.13
Phe^7	7.74	4.39	3.04, 2.81		2, 6H: 7.20, 3, 5H: 7.31
Phe^8	7.43	4.17	3.09, 3.05		2, 6H: 7.20, 3, 5H: 7.31
Gly^9	7.94	3.81, 3.57			
Leu^{10}	7.50	4.17	1.72	1.76	δCH_2: 0.96, 0.90
Met^{11}		4.44	2.35,2.06	2.69, 2.56	NH_2: 7.35, 7.20

n, non-measurable.

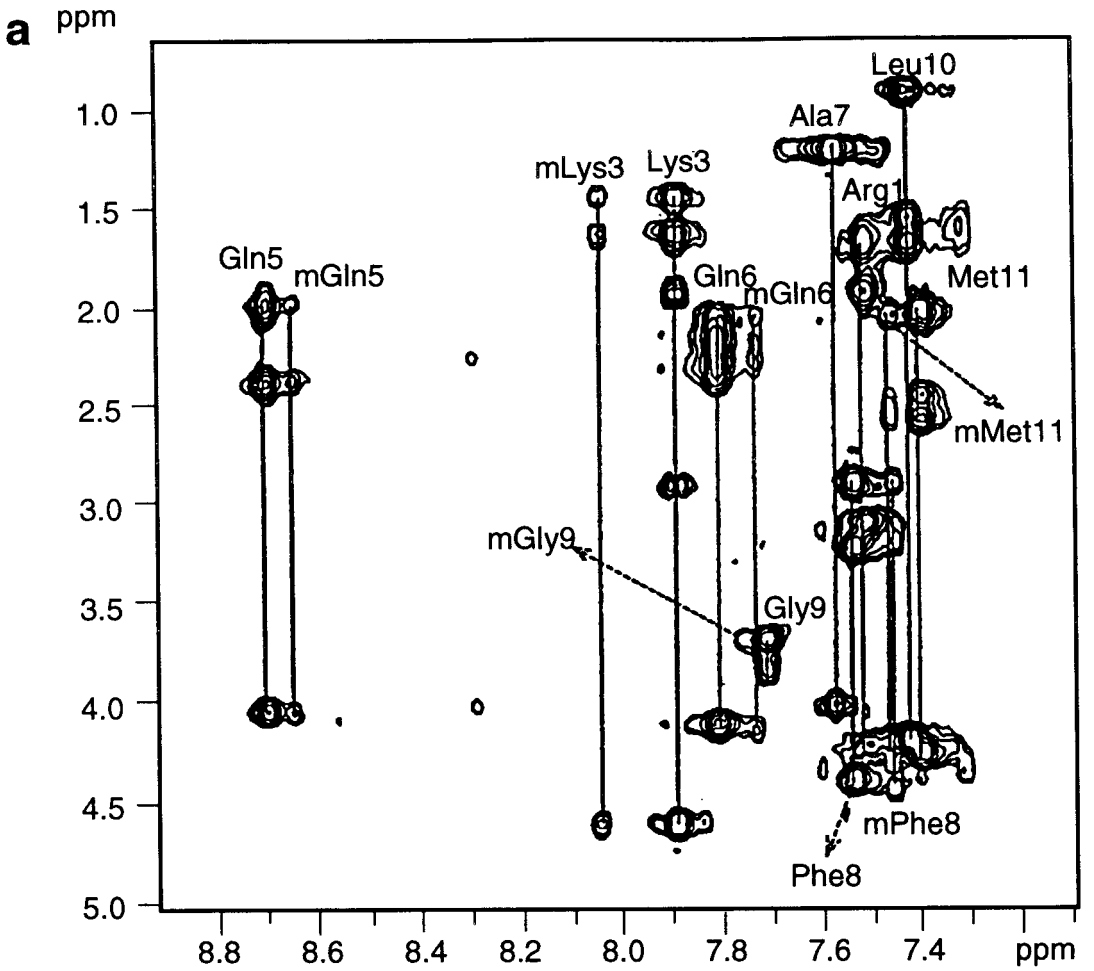

Figure 4 NMR data in 80:20 (v:v) ACN-d_3:TFE-d_2: (a) TOCSY spectrum of Ala^7-SP in the amide–aliphatic region; (b) ROESY spectrum of Ala^7-SP in the amide-C$^{\alpha}$H region; (c) TOCSY spectrum of Ca^{2+}-saturated Ala^7-SP (with 6 molar excess of Ca^{2+}) in the amide–aliphatic region.

binding curves were either shallow or the $\Delta\delta$ for some of the protons (e.g. Gln^6, Gly^9) changed sign midway so that the stoichiometry of binding was difficult to assess. Based on the CD data in pure TFE (Figure 1, top inset), we have assumed the predominant species at high Ca^{2+}:peptide ratio to be the 1:1 complex. It is interesting to note that Lys^3 in the *N*-terminal region of Ala^7-SP undergoes a much smaller change in NH chemical shift over a range of Ca^{2+} concentration when compared with SP. This would suggest the *C*-terminal region to be the plausible site for Ca^{2+} binding in this peptide. This is further supported by the relatively large $\Delta\delta$ observed for Gln^6, Gly^9 and Leu^{10}. Combined with the NOE connectivity data presented below, the Ca^{2+} titration data provide an insight into the residues involved in Ca^{2+} binding.

Coupling constants. The $^3J_{NH\text{-}\alpha H}$ coupling constants for key amide protons in SP and its 1:1 and 2:1 Ca^{2+} complexes were obtained from resolution-enhanced one-dimensional proton spectra supplemented by two-dimensional TOCSY spectral data. Because many of the line widths were relatively broad in the spectra of the SP:Ca^{2+} complexes, some resonances were either not measurable or the accuracy of measurement was low. The coupling constant data are listed in Table 3. For SP, the coupling constants for residues Gln^5 and Gln^6 and for Gly^9, Lys^{10} and Met^{11} ranged from 3.6 to 5.4Hz, which are values expected for peptide helices; residues in an ideal α-helix would have a $^3J_{NH\text{-}\alpha H}$ coupling constant of 4.0 Hz [31]. In the 1:1 and 2:1 Ca^{2+}:SP complexes, residues Gln^5-Leu^{10} and Phe^7-Leu^{10} had coupling constants suggestive of

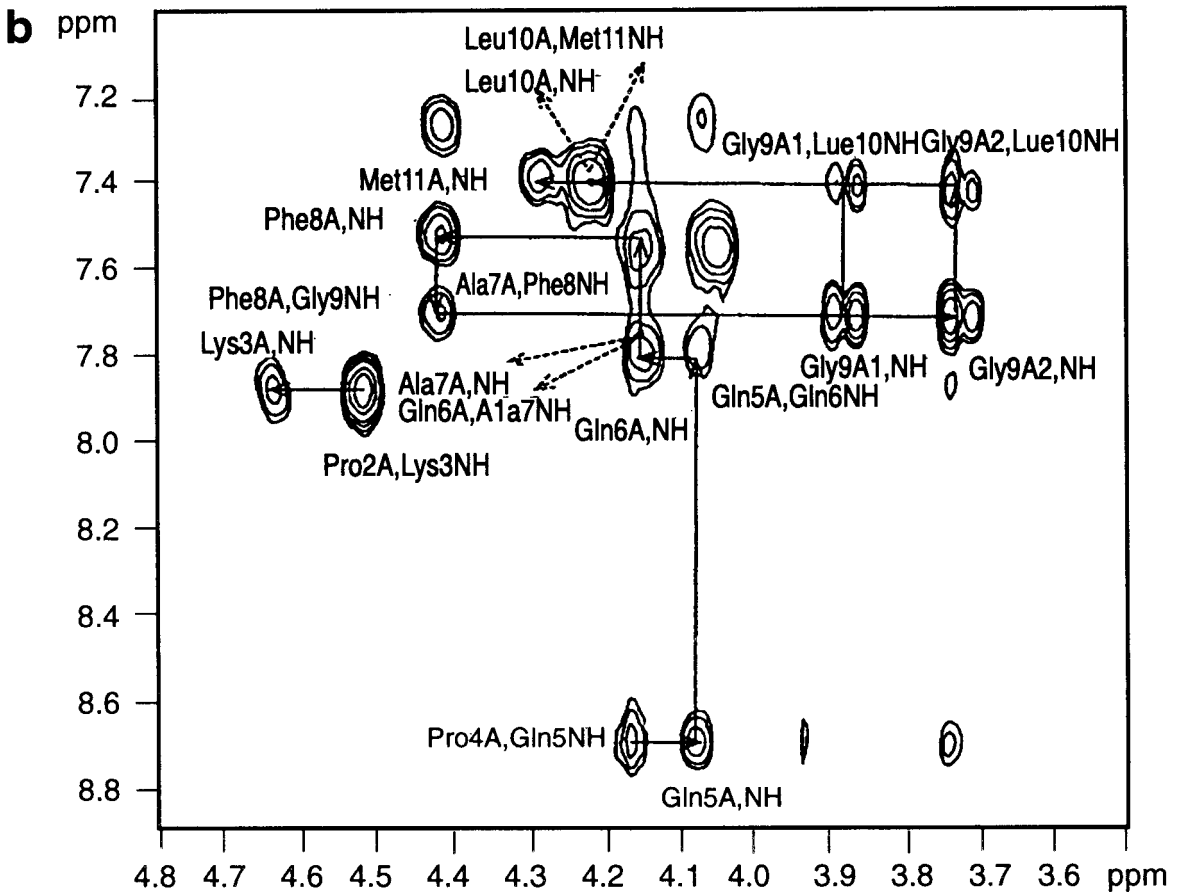

Figure 4 (*Continued*)

non-α helical regions. It is noticed that in both SP and its two Ca^{2+} complexes, the *N*-terminus had more non-helical residues than the *C*-terminus. The coupling constants of Ala^7-SP in the free and Ca^{2+}-bound forms are also shown in Table 3. Except Ala^7, all the residues between 5 and 9 in Ala^7-SP exhibited similar $^3J_{NH\text{-}\alpha H}$ value as in SP. Thus, the fragment of 5–9 in the molecule could be considered as the key secondary structural element related to its helical structure. Severe spin coupling and line broadening made the coupling constant estimates of Ca^{2+}-bound Ala^7-SP very approximate (data not shown).

NOE connectivities. NOESY and ROESY spectra (obtained with a mixing time of 200 ms and 300 ms) were used to obtain three-dimensional information by way of distance constraints in the peptides and their Ca^{2+} complexes. The effect of spin diffusion in the NOESY and ROESY spectra was negligible since the measured NOE and ROE volumes increased linearly with mixing time up to 400 ms, beyond which some non-linearity set in (data not shown).

A total of 41 *intra* and 51 *inter*residual NOEs were observed in SP, 23 *intra* and 61 *inter*residual NOEs in the 1:1 Ca^{2+}:SP complex and, 28 *intra* and 52 *inter*residual NOEs in the 2:1 Ca^{2+}:SP complex. Of particular interest was the observation of a grouping of certain medium range NOEs, which can be used to determine the presence of secondary structures, such as the α-helix, β-sheet or β-turn [31]. The NOE connectivities that are important in characterizing such secondary structures in SP, Ala^7-SP and their Ca^{2+} complexes are shown in Figures 8 and 9. (Owing to the line-broadening problem in NOESY spectra, ROE connectivities rather than NOEs are shown for Ca^{2+}-bound Ala^7-SP (Figure 9).) Four NH(i)–NH($i+2$), one NH(i)–NH($i+3$) and two αH(i)–NH($i+3$) NOE connectivities were present in SP (Figure 8). This strongly supports the presence of a helical structure in this region of the peptide. For the 1:1 Ca^{2+}:SP complex, significant medium-range NOE connectivities were observed in residues ranging from Pro^4 to Met^{11}. Among them, NOEs showing

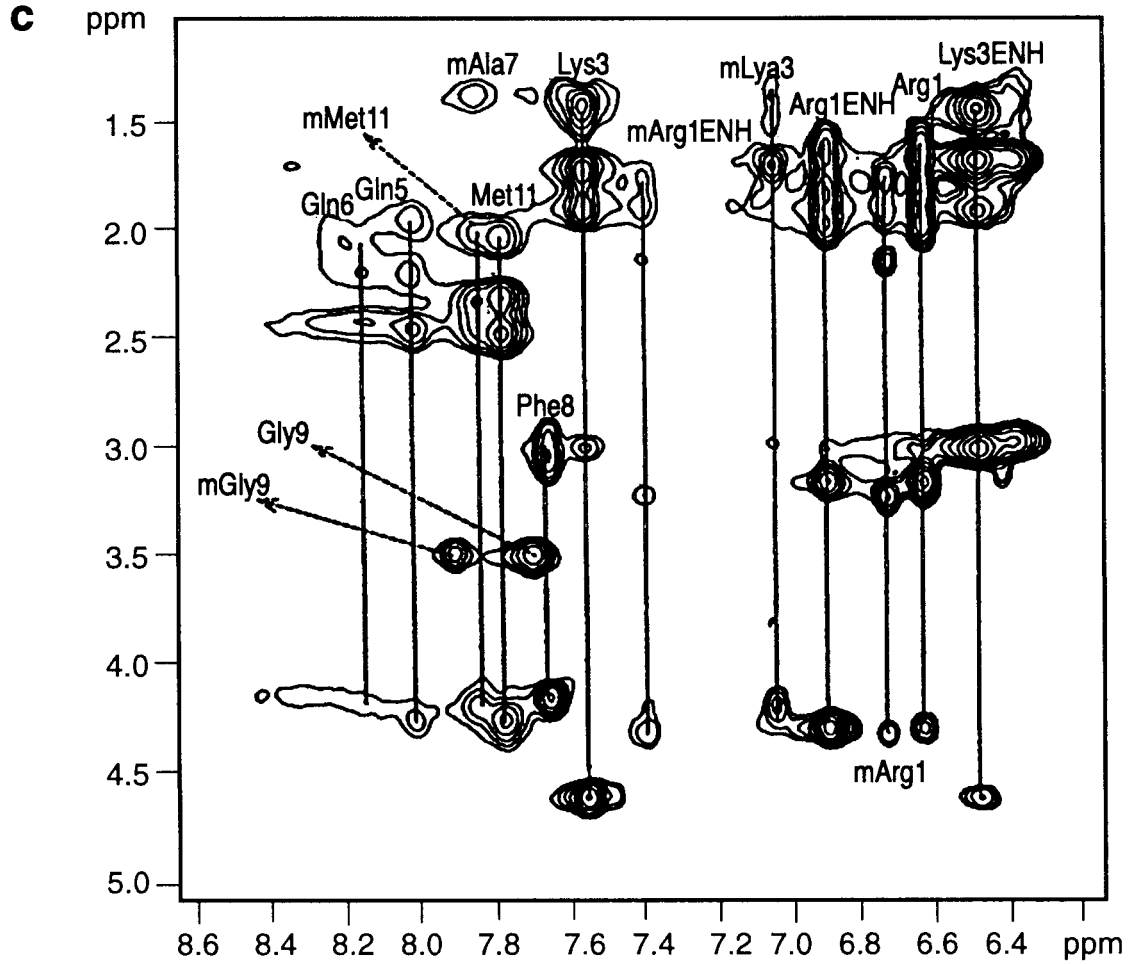

Figure 4 (*Continued*)

seven αH(i)–NH($i+2$), four βH(i)–NH($i+2$), two NH(i)–NH($i+2$), three αH(i)–NH($i+3$) and one αH(i)–βH($i+3$) connectivies suggested a 3_{10}-helix, although two αH(i)–NH($i+4$) NOEs in this region indicated the possibility of an α-helix. Addition of two molar equivalents of Ca^{2+} to SP caused a reduction in secondary structural NOE cross-peaks (Figure 3(c) and Figure 8(c)). However, the grouping of three weak αH(i)–NH($i+2$) NOEs, two weak αH(i)–NH($i+3$) NOEs, and one weak αH(i)–NH($i+4$) NOE indicated an α-helix in the region between Gln^5 and Leu^{10} in the 2:1 Ca^{2+}:SP complex. In SP and in its two Ca^{2+} complexes, the $^3J_{NH\text{-}\alpha H}$ coupling constants in the *C*-terminal region were less than 6.5 Hz (Table 3), supporting the presence of a helical structure in this region.

Many ROE signals were observed in the ROESY spectrum of Ala^7-SP in the free form. Of these, a total of 22 *intra* and 97 *inter*residual ROEs were used for the analysis and three-dimensional structural modeling of Ala^7-SP. Four medium NH(i)–NH($i+2$) ROEs and three medium αH(i)–NH($i+3$) ROEs were found in fragment 6–11 in ROESY spectrum for Ala^7-SP, which strongly supported the presence of the α- or 3_{10}-helical structure in this region of the peptide (Figure 9). However, because $^3J_{NH\text{-}\alpha H}$ coupling constants for residues Phe^8 and Met^{11} are more than 6.5 Hz, this region may be undergoing an equilibrium between helical and other turn or loop-like conformations. In addition, three weak long-range *inter*-residue αH(i)–NH($i+6$) ROEs existed within residues 2–11, which suggests that a compact structure is still the dominant one and may be in structural equilibrium with other minor conformers. Compared with the free peptide, a far less number of *inter*residue ROEs were found in the ROESY spectrum for Ca^{2+}-saturated Ala^7-SP. Some ROE connectivities are shown in Figure 9 that indicate that

the *C*-terminal may contain an equilibrium mixture of predominantly β-turn-like structures and a small population of helical structure around residues 6–11. In contrast, the ROEs suggest that the *N*-terminal region has a more flexible structure.

Based on the observation of NOE and ROE connectivities alone it is difficult to differentiate between an α-helix and a 3_{10}-helix [31]. For the quantitative evaluations of structures of SP and its 1:1, 2:1 Ca^{2+}-bound complexes and of Ala^7-SP and its 1:1 Ca^{2+} complex, the NOE and ROE data were used to obtain *inter*proton distance constraints, which could then be used in molecular modeling by computation. Towards this, the *intra* and *inter*residual NOE and ROE cross-peaks were volume-integrated. The strengths of the volume integrals were then related to threshold distance ranges as: 1.8–2.5 Å (strong), 1.8–3.3 Å (medium), 1.8–4.0 Å (weak) and 1.8–5.0 Å (very weak), by comparison with the known distances of pairs of connected protons, which had well resolved NOE and ROEs (see the Methods section). The lowest distance, 1.8 Å, is the sum of the van der Waals radii of two protons.

Molecular Modeling

For the free peptides as well as their Ca^{2+} complexes, two MCM trajectories were calculated with starting conformations corresponding to the ideal left-handed and right-handed α-helices (Table 4). The trajectory was terminated when the last 500

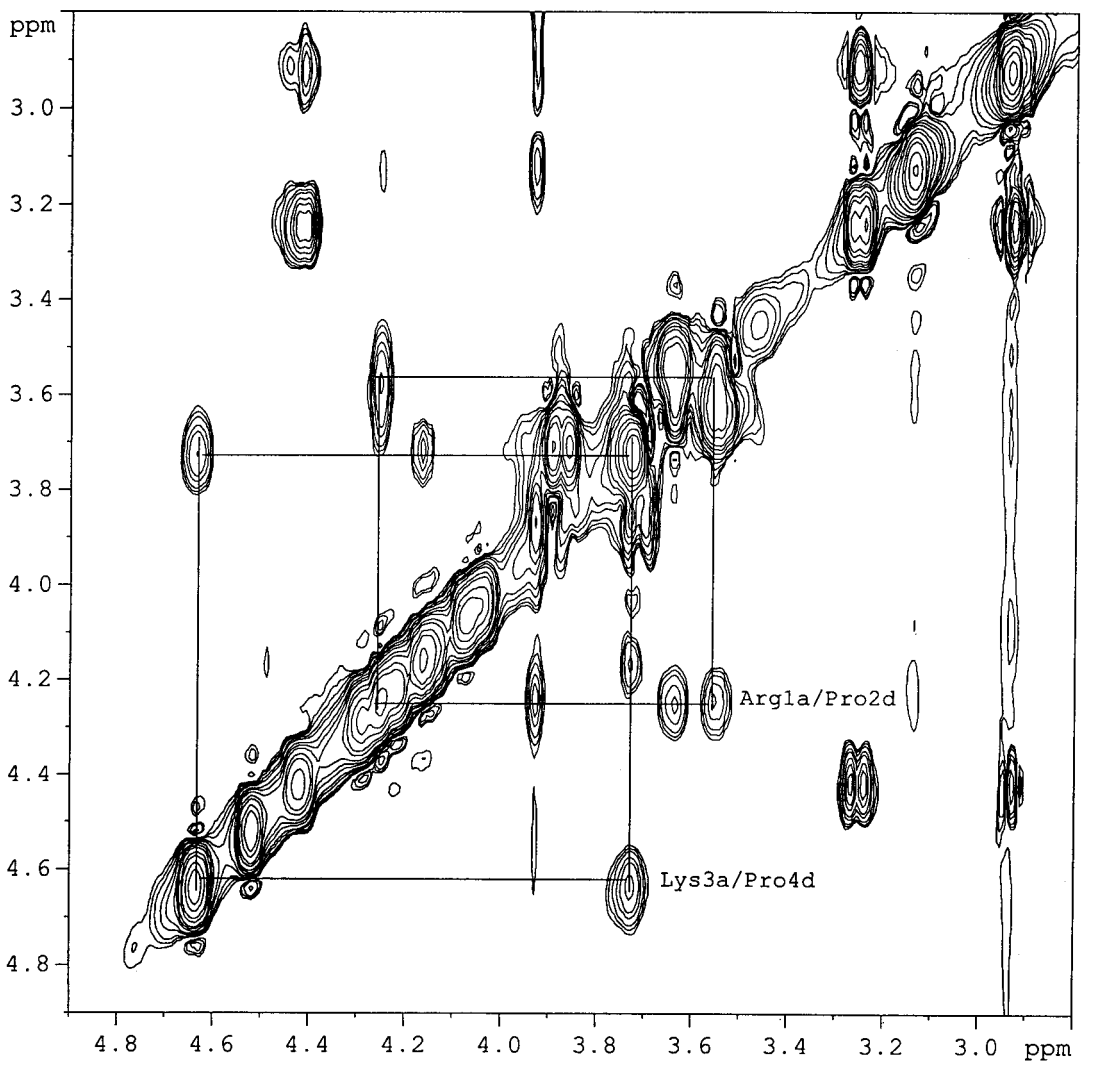

Figure 5 ROESY spectrum of Ala^7-SP in 80:20 (v:v) ACN-d_3:TFE d_2 in the amide-C$^{\alpha}$H region showing the predominance of *trans* conformation around X-Pro bonds.

Table 2 Proton Chemical Shift (δ) Assignments for Ala^7-SP and its Ca^{2+} Complex in 80:20 (v:v) ACN-d_3:TFE-d_2 at 300 K

Peptide/residue	NH	αH	βH	γH	Other
Ala^7-SP					
Arg^1	7.51	4.26	1.95, 1.91	1.72, 1.62	δCH_2: 3.14
Pro^2		4.53	2.24, 2.02	1.94, 1.88	δCH_2: 3.65, 3.56
Lys^3	7.88	4.64	1.96, 1.64	1.45	δCH_2: 1.65, εCH_2: 2.95
Pro^4		4.17	2.30, 2.07	1.98, 1.94	δCH_2: 3.75
Gln^5	8.69	4.08	2.05, 1.98	2.42	δNH_2: 6.62, 6.05
Gln^6	7.80	4.15	2.19, 2.04	2.36, 2.30	δNH_2: 6.77, 6.19
Ala^7	7.73	4.16	1.21		
Phe^8	7.53	4.42	3.25, 2.94		
Gly^9	7.70	3.88, 3.72			
Leu^{10}	7.41	4.23	1.59, 1.22	1.71	δCH_2: 0.93, 0.88
Met^{11}	7.39	4.29	2.11, 2.03	2.61, 2.49	NH_2: 6.82, 6.31
Ala^7-SP+Ca^{2+}					
Arg^1	6.62	4.31	2.02, 1.89	1.76, 1.63	δCH_2: 3.19
Pro^2		4.50	2.26, 2.02	1.93	δCH_2: 3.68, 3.60
Lys^3	7.55	4.63	1.96, 1.80	1.49	δCH_2: 1.71, εCH_2: 3.02
Pro^4		4.43	2.26	2.01	δCH_2: 3.76, 3.68
Gln^5	8.01	4.27	2.21, 2.16	2.51	δNH_2: 6.62, 6.11
Gln^6	8.17	4.21	2.21, 2.16	2.44	δNH_2: 6.46, 6.11
Ala^7	7.56	4.08	1.39		
Phe^8	7.69	4.18	3.11, 2.99		2, 6H: 7.21, 3, 5H: 7.33
Gly^9	7.65	3.87, 3.52			
Leu^{10}	n	4.15	1.75, 1.59	1.75	δCH_2: 0.94, 0.90
Met^{11}	7.77	4.28	2.05	2.50, 2.34	NH_2: 6.93, 6.48

n, non-measurable.

energy minimization did not lower the energy of the best MEC found nor added a new MEC to the conformational stack. Each trajectory converged to a conformational region (denoted by letter codes according to Zimmermann *et al.* [37]), where a maximal number of NOE constraints were satisfied. All the NOE constraints were never matched simultaneously in any one MEC. This is to be expected in light of the possibility of several low-energy conformers existing in equilibrium with the global (lowest-energy) MEC. Trajectories that started from the regular helical structures retained their original conformations in central residues whereas *N*- and *C*-termini of the helices were usually disordered.

Table 3 $^3J_{NH\text{-}\alpha H}$ Coupling Constants (in Hz) of SP, its Ca^{2+} Complexes and Ala^7-SP in 80:20 (v:v) ACN-d_3:TFE-d_2 at 300 K

Residue	SP	1:1 Ca^{2+}:SP	2:1 Ca^{2+}:SP	Ala^7-SP
Lys^3	7.5 ± 0.1	8.7 ± 0.5	7.9 ± 0.5	7.4 ± 0.1
Gln^5	4.2 ± 0.2	4.8 ± 0.6	8.0 ± 0.3	3.8 ± 0.3
Gln^6	5.1 ± 0.3	n	n	5.2 ± 0.4
Phe^7	7.2 ± 0.6	n	5.5 ± 0.4	
Ala^7				5.4 ± 0.4
Phe^8	6.2 ± 0.5	5.3 ± 0.5	4.5 ± 0.7	6.8 ± 0.3
Gly^9	5.4 ± 0.1	4.2 ± 0.6	5.2 ± 0.4	4.6 ± 0.6
Leu^{10}	3.6 ± 0.2	5.4 ± 0.5	3.6 ± 0.6	5.9 ± 0.5
Met^{11}	4.7 ± 0.2	6.1 ± 0.4	7.5 ± 0.6	7.2 ± 0.3

n, non-measurable.

The right-handed α-helix was found to be the optimal MECs in SP and SP:Ca^{2+}, whereas the left-handed helix was the most preferable in SP:2Ca^{2+} complex. The latter may account for the reversal in the sign of the 220 nm CD band of the 2:1 Ca^{2+}:SP complex (Figure 1, curve d). In the case of the Ca^{2+} complexes, we used, as additional constraints, the magnitudes of chemical shift changes undergone by the NH and αCH protons during the titration of SP with Ca^{2+} (Figure 7) and combined these with the NOE constraints to arrive at the best MECs. In the case of the Ca^{2+} complexes of Ala^7-SP, because of line broadening and the limited number of ROEs observed, the input of the Ca^{2+} titration data was particularly useful in the modeling process. The torsional angles of the best MECs found for SP, 1:1 SP:Ca^{2+}, and 1:2 SP:Ca^{2+}, Ala^7-SP and 1:1 Ala^7-SP:Ca^{2+} are given in Table 4 and the Ca^{2+}–oxygen contacts are given in Table 5, which also shows the *C*-terminal region in SP binding the Ca^{2+} ion first before the *N*-terminal part. The computed structures are shown in the color plate (a)–(e). Data pertaining to calculated and NOE-derived *inter*proton distances were also obtained but not shown. Compared with SP, the *N*-terminal region of Ala^7-SP is less ordered (see plate) in agreement with the NOE data (Figures 8 and 9) and with the lower helix content observed in the CD spectrum of this peptide (Figure 1). There are also differences between the 1:1 Ca^{2+} complexes of SP and Ala^7-SP in terms of the torsional angles (Table 4) and residues that participate in Ca^{2+} chelation (see plate). Since the only difference between the two peptides is the absence of the aromatic ring in Ala^7-SP, it is likely that the Phe ring helps stabilize the helix in the *N*-terminal region of SP by some long-range interaction and also helps in the binding of the second Ca^{2+} in this region.

DISCUSSION

Substance P is one of the most studied peptide hormones for its structure in a variety of solvents. Of special import are the structures determined in

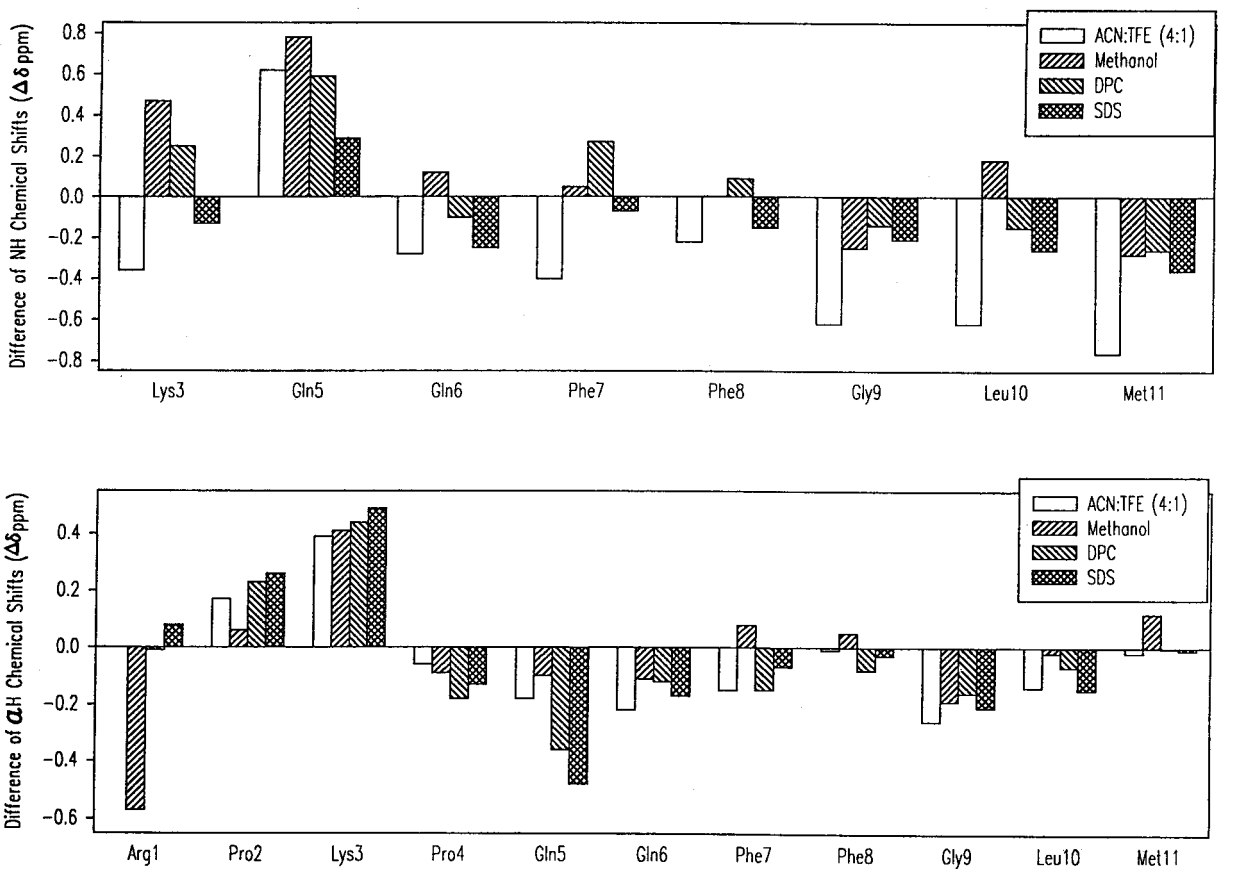

Figure 6 Chemical shift differences in NH and $C^{\alpha}H$ protons of SP in non-polar solvents and lipid micelles. Sources of the data are indicated in the text.

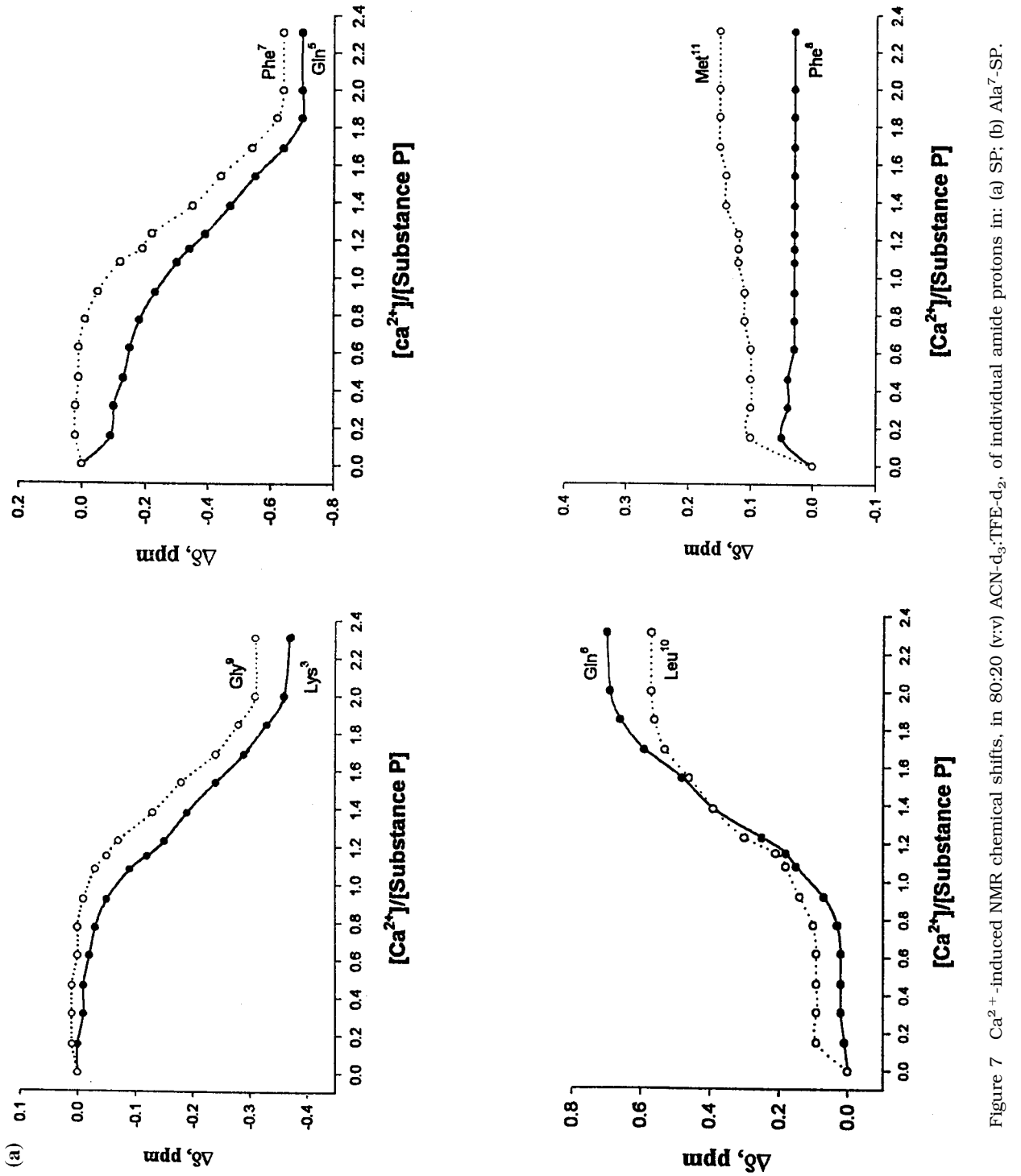

Figure 7 Ca^{2+}-induced NMR chemical shifts, in 80:20 (v:v) ACN-d_3:TFE-d_2, of individual amide protons in: (a) SP; (b) Ala^7-SP.

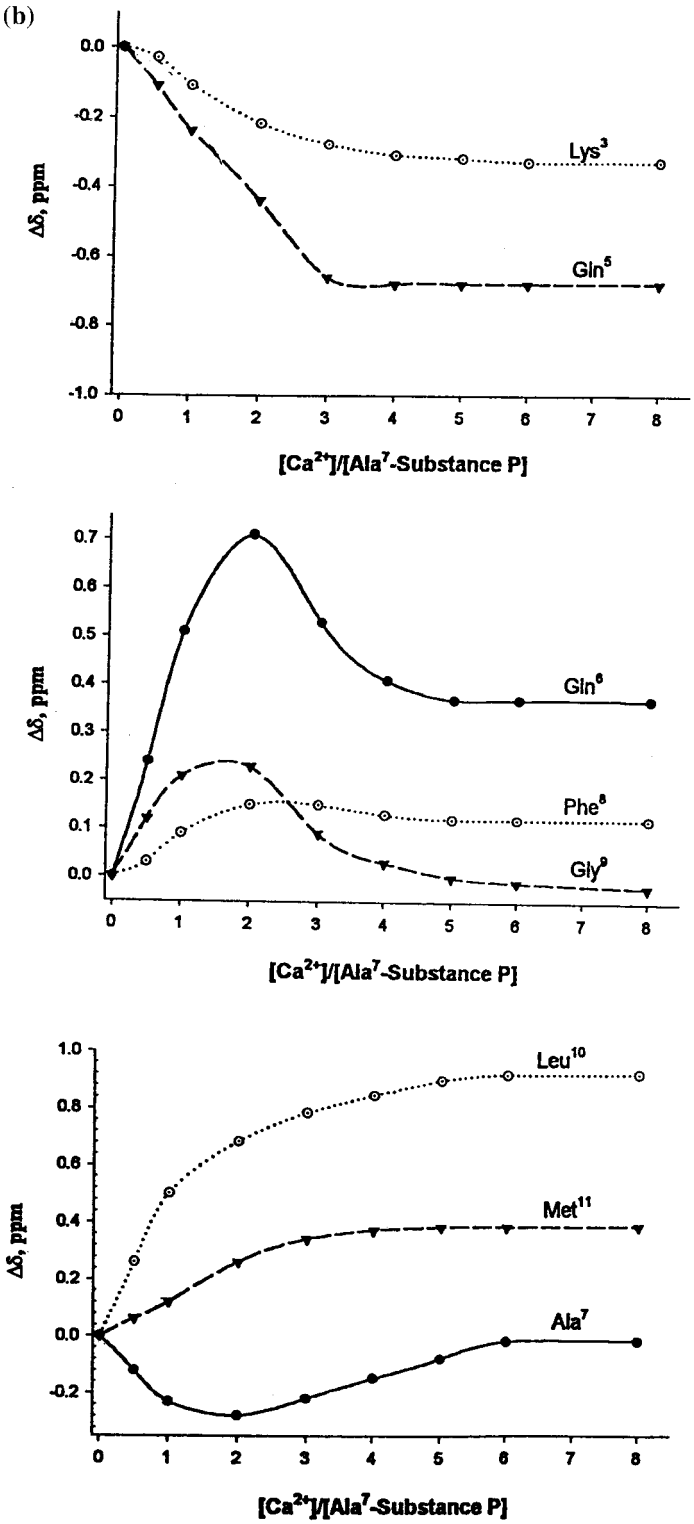

Figure 7 (*Continued*)

synthetic lipid micelles and bilayers, as these provide the peptide the low-dielectric constant milieu of the biological membrane, which, unlike water, would support an ordered peptide conformation. Based on these data and on the assumption that the structure of a peptide hormone in the lipid milieu would represent the receptor-bound conformation or a lipid-bound intermediate form of the peptide [3,14], models for membrane bound SP have been advanced by several groups of workers [3,8–10,12,15,18–25]. We have, in our laboratory, regarded the interaction of the peptide hormone with extracellular Ca^{2+} as an additional factor that would modify the conformation of the lipid-bound hormone [26]. That the Ca^{2+}-bound structure is biologically relevant has been demonstrated by our showing a correlation between the activities of GnRH analogs and their extent of interaction with

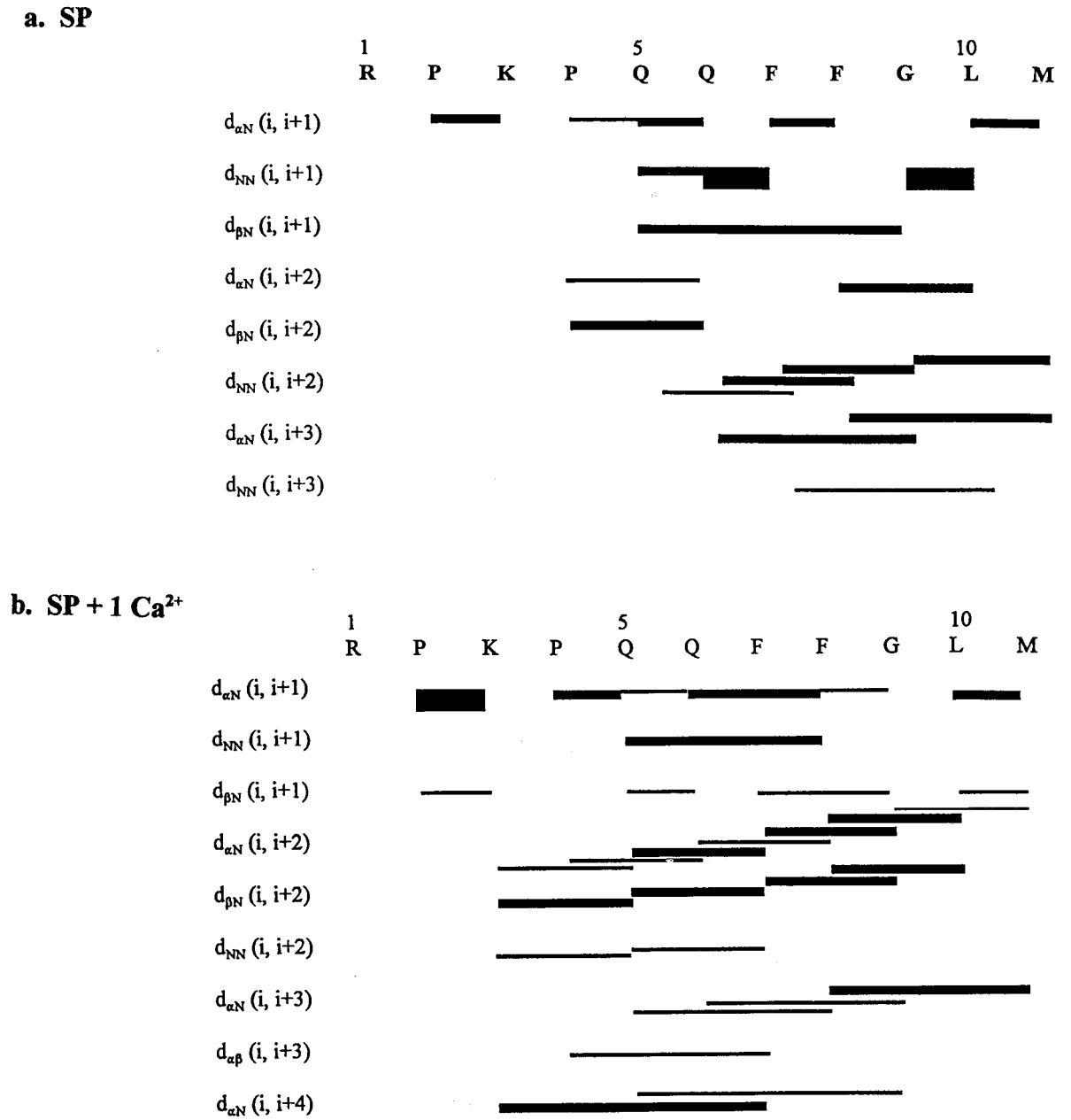

Figure 8 NOE connectivities in: (a) SP; (b) 1:1 Ca^{2+}:SP complex; and (c) 2:1 Ca^{2+}:SP complex.

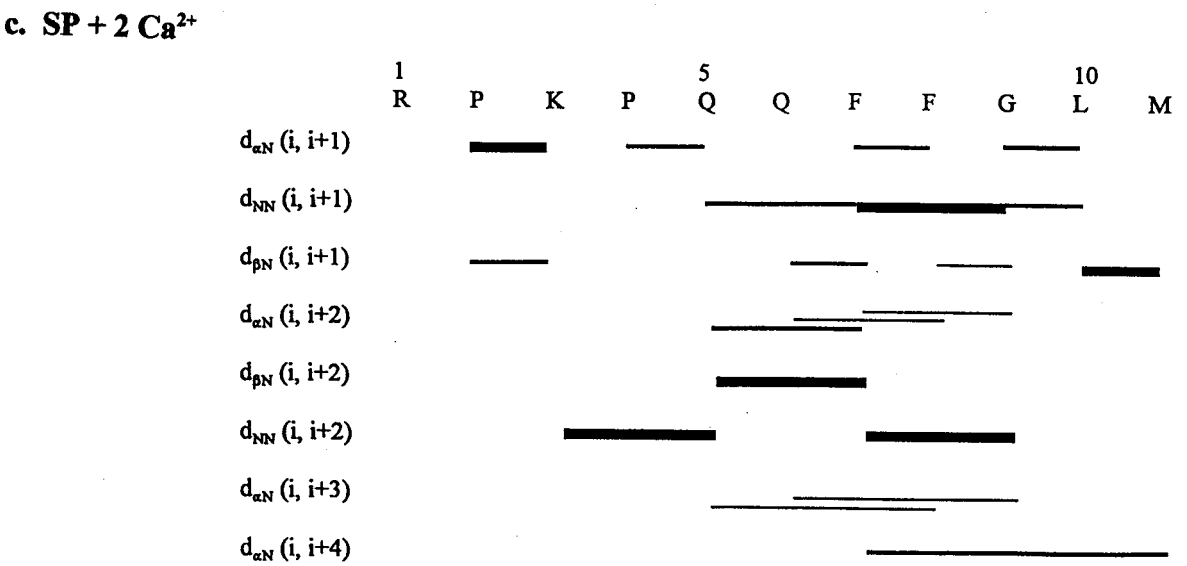

Figure 8 (*Continued*)

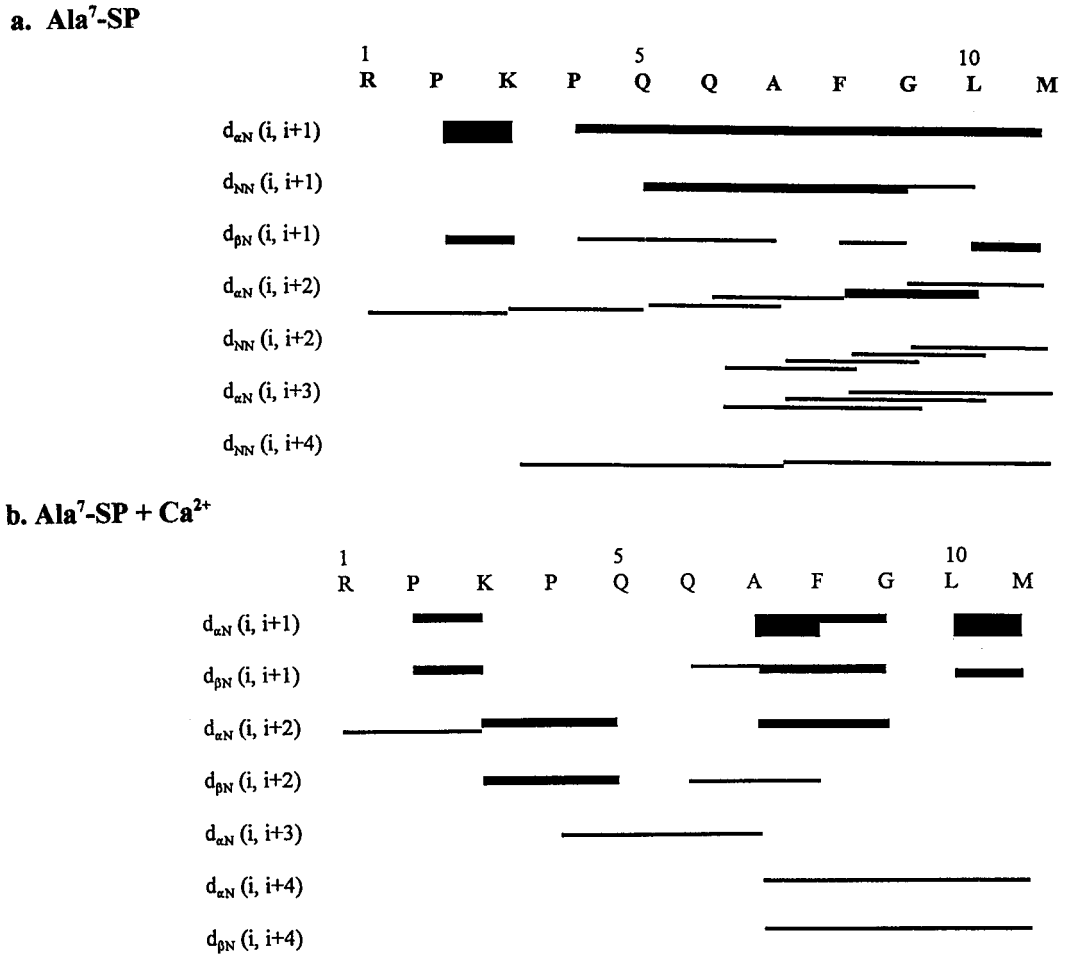

Figure 9 NOE connectivities in: (a) Ala^7-SP, and (b) 1:1 Ca^{2+}:Ala^7-SP complex.

Table 4 Torsional Angles (τ)[a] of the Lowest-Energy MECs[b] of the Free and Ca^{2+}-bound Forms of SP and Ala^7-SP and Standard Deviations (σ) from the Mean Torsions Calculated Over all the MECS Accumulated in the Stack[c]

Residue	Torsion	SP						Ala^7-SP			
		Free		Ca^{2+}		$2Ca^{2+}$		Free		Ca^{2+}	
		τ (°)	σ(118)[d] (°)	τ (°)	σ(178)[e] (°)	τ (°)	σ(173)[d] (°)	τ (°)	σ(68)[f] (°)	τ (°)	σ(471)[d] (°)
Arg^1	Ψ	117	4	153	7	155	5	156	25	145	30
	ω	−177	2	175	2	172	5	168	5	176	6
	χ^1	−169	3	−74	43	−79	64	57	85	65	28
	χ^2	176	7	−165	19	−87	53	−178	10	−166	13
	χ^3	−176	54	−62	61	−179	91	−172	64	177	106
	χ^4	168	4	−92	71	178	61	86	46	86	35
Pro^2	ϕ	−36	2	−73	4	−44	8	−63	11	−74	8
	Ψ	−64	5	−20	7	−74	4	155	12	80	26
	ω	−170	2	−171	2	163	4	−174	3	179	4
	χ^4	15	4	−13	3	18	18	−20	13	−8	15
	χ^3	−38	4	35	2	−37	35	36	31	31	31
	χ^1	−50	2	27	3	−44	29	19	31	26	28
Lys^3	ϕ	−61	4	−71	5	48	4	−140	7	−68	9
	Ψ	−63	5	−47	3	79	2	−53	4	145	4
	ω	−176	3	172	4	−159	5	159	6	167	7
	$\chi 1$	167	37	−70	30	−172	46	−53	41	72	52
	χ^2	158	13	162	62	171	68	−171	82	−160	26
	χ^3	179	30	−81	51	174	52	174	35	−70	56
	χ^4	63	9	−179	88	178	84	66	63	106	72
Pro^4	ϕ	−54	2	−36	5	−17	8	−54	7	−83	9
	Ψ	−43	5	−54	3	89	9	−64	8	−176	23
	ω	179	3	−176	2	−179	2	−172	3	172	7
	χ^4	−21	13	2	12	−16	12	−23	10	2	8
	χ^3	32	20	−19	23	−8	13	29	19	16	16
	χ^1	11	14	−37	20	−55	2	10	17	23	17
Gln^5	ϕ	−50	4	−60	2	63	5	−56	4	−72	6
	Ψ	−64	4	−54	2	−82	9	−33	4	93	11
	ω	−162	4	−175	1	−150	4	−177	2	−170	6
	χ^1	177	5	−177	2	−176	41	−153	9	−156	62
	χ^2	−172	5	62	1	157	2	70	21	−68	64
	χ^3	0	12	101	4	110	27	−102	53	−61	125
Gln^6	ϕ	−76	5	−89	4	63	4	−68	5	−75	4
	Ψ	−24	3	−78	4	−74	10	−47	4	−171	3
	ω	−172	4	−146	4	−159	6	177	3	167	3
	χ^1	78	59	−126	37	−53	6	−166	50	−53	3
	χ^2	−176	45	−65	71	167	7	−176	36	−156	54
	χ^3	96	102	10	78	−100	16	−94	107	114	113
Phe/Ala^7	ϕ	−55	4	−81	5	10	6	−61	2	65	4
	Ψ	−37	4	−49	8	77	2	−37	5	−160	4
	ω	172	2	176	3	175	3	−177	3	178	5
	χ^1	172	5	−62	5	−177	56				
	χ^2	76	81	122	5	−110	72				

Table 4 (*Continued*)

Residue	Torsion	SP						Ala^7-SP			
		Free		Ca^{2+}		$2Ca^{2+}$		Free		Ca^{2+}	
		τ (°)	$\sigma(118)^d$ (°)	τ (°)	$\sigma(178)^e$ (°)	τ (°)	$\sigma(173)^d$ (°)	τ (°)	$\sigma(68)^f$ (°)	τ (°)	$\sigma(471)^d$ (°)
Phe^8	ϕ	−106	4	−84	5	53	2	−71	6	−53	6
	Ψ	−24	5	133	2	93	2	−31	7	161	6
	ω	−165	4	−177	1	166	5	177	2	179	3
	χ^1	73	8	174	36	−54	57	−177	16	−64	64
	χ^2	84	47	78	87	116	69	80	80	119	75
Gly^9	ϕ	−68	3	65	2	70	1	−74	7	83	3
	Ψ	−83	9	161	6	−168	6	−39	6	177	4
	ω	−166	3	−178	3	−179	2	176	4	−172	2
Leu^{10}	ϕ	−83	5	−67	3	−65	2	−67	3	−64	2
	Ψ	−23	9	−95	7	−73	4	−35	6	158	3
	ω	174	10	−176	5	−171	2	176	2	179	2
	χ^1	−76	5	−83	57	−69	27	−68	55	−63	13
	χ^2	−60	8	−70	85	156	115	160	48	165	26
Met^{11}	ϕ	−154	33	−110	5	−55	5	−68	7	58	3
	Ψ	−53	5	−60	11	143	14	−42	2	177	12
	χ^1	−172	66	−67	77	−172	36	−174	41	−53	45
	χ^2	−179	10	−62	62	172	44	174	36	−174	55
	χ^3	−80	94	−64	49	179	58	80	52	−179	58

[a] Torsions involving CH_3, NH_2, NH3 and COOH groups are not shown.
[b] Found by the stochastically restrainable Monte Carlo minimization protocol, see the Methods section.
[c] The number of the MECs is shown in parenthesis.
[d,e,f] The stack includes MECs with the energy up to 15 ([d]), 10 ([e]), or 7 ([f]) kcal mol^{-1} from the apparent global minimum.

Ca^{2+} [43] and by observing a marked difference in Ca^{2+} binding between oxytocin and vasopressin [39]. In the present study, we have looked at the interaction with Ca^{2+} of SP and its inactive analog Ala^7-SP in a lipid-mimetic solvent, ACN-TEF by CD and NMR and have delineated their Ca^{2+}-bound structures by NMR and molecular modeling.

A large number of the structure–activity studies on SP are based on measurements on chemically modified forms of the parent hormone [44–46]. However, such studies tend to be empirical and do not provide a clue to the bioactive (receptor-bound) conformation of SP. An exception is the studies of Kessler and his co-workers [47–49], who synthesized potent agonists of SP by backbone cyclization of the *C*-terminal part of the hormone and determined their structures by NMR and computational methods. The cyclic portion of these peptides was compact, while the linear portion (-Gly-Leu-Met-NH_2) was extended. The side chains of the adjacent Phe residues showed conformational averaging with a preference for the −60 and −180° rotomers. Since Leu-Met-NH_2 is also essential for bioactivity of SP, the authors proposed constraining this portion of SP as well to arrive at the receptor-bound conformation [47]. These studies contribute to realizing the ultimate goal of designing potent SP agonists and antagonists as they provide clues to the receptor-bound conformation of the linear, native hormone. It will also be valuable to obtain such information more directly through comparative studies of the structures of native SP and its linear agonist analogs. Such data have, however, not been available. In this study, we have characterized the conformations of SP and Ala^7-SP both in the absence and presence of Ca^{2+} in a lipid-mimetic solvent. That SP (and many other hormones) binds Ca^{2+} inside the lipid bilayer is clearly evident from

the ability of SP and the *C*-terminal peptide SP(7–11) to carry the ion across the lipid bilayer of a synthetic liposomes suspended in an *aqueous* buffer medium [17]. Using Fourier transform infrared spectroscopy, Choo *et al.* [21] found no evidence for the interaction of SP, neither with lipid micelle or bilayer nor with Ca^{2+} in the presence of the lipid. Instead, they observed only peptide aggregation. This is in sharp contrast to the CD and NMR observations from other laboratories [9,23–25]. It is likely that the relatively high concentration of SP (7.4 mM) used by Choo *et al.* [21] could have caused peptide aggregation. Also, Ca^{2+} addition causes aggregation of negative lipids (even in the absence of the peptide) so that the authors' failure to observe the effect of Ca^{2+} addition on SP structure in negatively charged lipids is to be expected. Choo *et al.* [21] have concluded that the primary sequence of a peptide hormone and not its preferred conformation in the lipid milieu is responsible for receptor binding. This is in obvious contradiction to the findings from many laboratories.

Our present results show that SP and its Ala^7 analog assume an essentially helical structure in the non-polar medium particularly in the *C*-terminal 'message' region. However, a major difference exists in their interaction with Ca^{2+}. While the native hormone exhibits a stepwise binding of two Ca^{2+} ions, the Ala^7 analog is capable of binding only one Ca^{2+} ion. (It is likely that Ala^7-SP may bind a second Ca^{2+} ion with too weak an affinity to be quantitatively significant.) Interestingly, in both peptides, Ca^{2+} is bound at the initially helical *C*-terminal region involving residues 6–11. However, the structures of the resulting Ca^{2+} complexes are substantially different (Table 4 and plate). Also, in the native hormone but not in the analog peptide, Ca^{2+} binding at the *C*-terminal region facilitates the binding of another ion at the *N*-terminal region (residues 1–5). The *C*-terminal pentapeptide region of SP is known to bind to the receptor and exhibit receptor selectivity [4,5]. We have earlier observed that a peptide comprising the *C*-terminal region of SP can bind one Ca^{2+} while the peptide containing the *N*-terminal residues is not capable of binding the ion [17]. In light of these data, the reason for the poor bioactivity of Ala^7-SP would appear to lie in the dissimilarity between the conformations of the 1:1 Ca^{2+} complexes of this peptide and SP (see plate), which, in turn, results in the inability of the Ala^7-SP:Ca^{2+} complex to induce significant binding of a second Ca^{2+} ion at the *N*-terminal. Recently, Kiere and his co-workers [23,25] have made detailed NMR studies on SP bound to lipid micelles and have concluded that the region between residues 6 and 11 in the *C*-terminal part of SP is inserted into the lipid bilayer while the *N*-terminal region (residues 1–5) lies on the membrane surface. The peptide binding site in SP receptor presumably lies partly inside the transmembrane helical region and partly in the extracellular loop region of the receptor [50]. In light of our data, it would appear that the Ca^{2+}-bound *C*-terminal region of SP may be embedded inside the transmembrane helical region of the SP receptor, while the Ca^{2+}-bound *N*-terminal region of SP might interact with the extracellular loop residues. The distance between the Ca^{2+} ions in the structure of 2:1 Ca^{2+}:SP (see plate) is about

Table 5 Ca^{2+}-Oxygen Contacts in the Optimal MECs of SP and Ala^7-SP with Ca^{2+}

Complex	Peptide oxygen	Distance (Å)	Ca^{2+} number[a]
SP:Ca^{2+}	O_Lys^3	3.8	
	O_Pro^4	2.5	
	O_Gln^5	2.6	
	O_Gln^6	2.4	
	O_Phe^8	2.6	
	O_Gly^9	2.5	
	O_Leu^{10}	2.7	
SP:2Ca^{2+}	O_Arg^1	2.8	2
	O_Pro^2	2.5	2
	O_Lys^3	2.8	2
	O_Gln^5	2.7	2
	Oε_Gln^6	2.5	2
	Oε_Gln^5	2.8	1
	O_Gln^6	2.5	1
	O_Phe^7	2.6	1
	O_Phe^8	3.1	1
	O_Gly^9	2.6	1
	O_Leu^{10}	2.7	1
	O_Met^{11}	2.5	1
Ala^7-SP:Ca^{2+}	Oε_Gln^5	2.5	
	O_Gln^5	2.6	
	O_Gln^6	2.8	
	O_Ala^7	2.8	
	O_Phe^8	2.6	
	O_Gly^9	2.5	
	O_Leu^{10}	2.5	
	O_Met^{11}	2.5	

[a] This refers to the sequence of binding, the *C*-terminal residues being involved in the binding of the first Ca^{2+}.

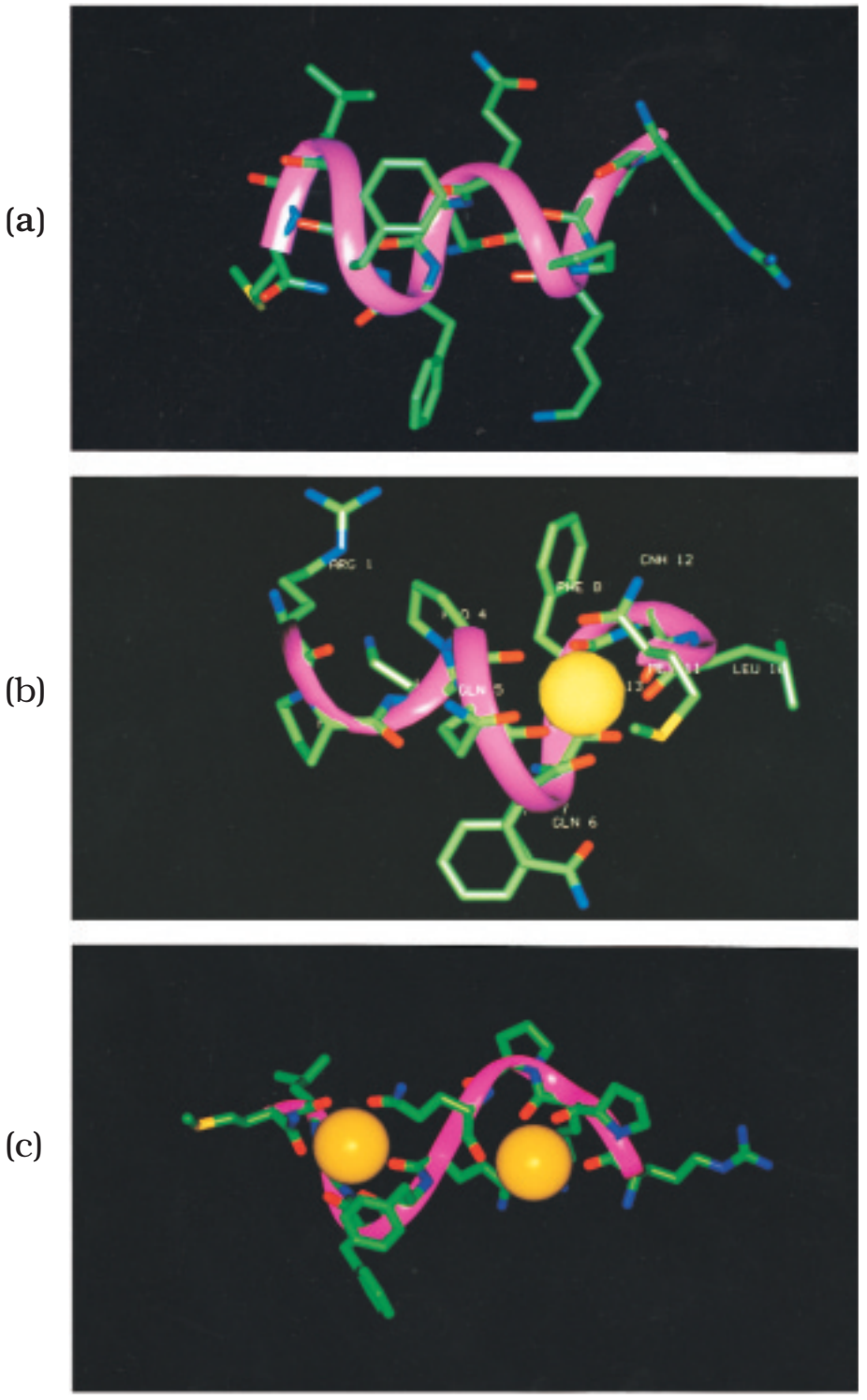

Plate 1 Minimum-energy conformations of a) SP; b) 1:1 Ca^{2+}:SP complex; c) 2:1 Ca^{2+}:SP complex; d) Ala^{7}-SP, and e) 1:1 Ca^{2+}:Ala^{7}-SP complex. These were computed using distance constraints derived from NOE and ROE data as well as from proton chemical shift changes in the peptide caused by Ca^{2+} addition.

(d)

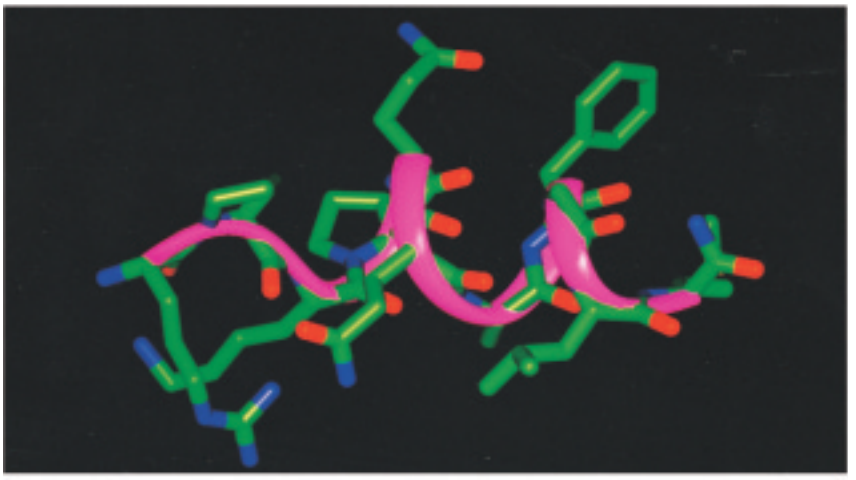

(e)

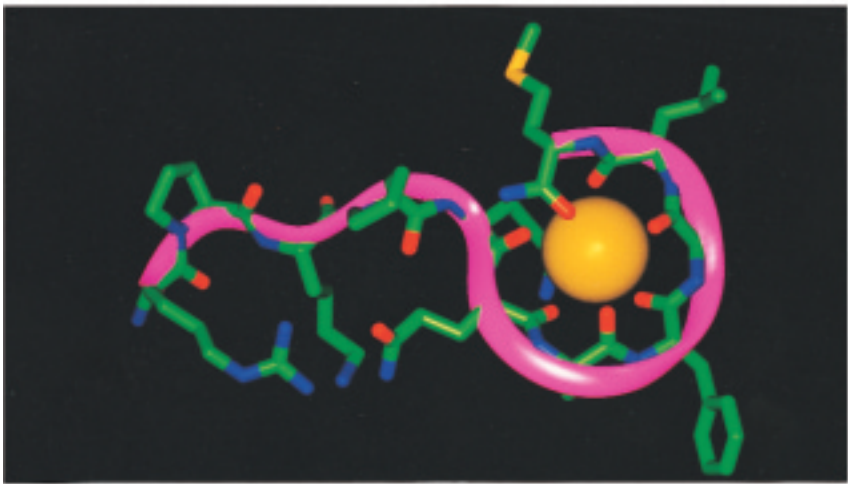

Plate 1 Continued.

7–8 Å, which, interestingly, is also maintained in the Ca^{2+}-bound forms of oxytocin [39] and μ-opioid agonist peptides [34]. The peptide-bound Ca^{2+} ions may interact with suitably placed acidic residues in the transmembrane and extracellular regions of receptors. A mechanism by which such an interaction could occur and lead to signal transduction in G-protein-coupled receptors has recently been proposed by us [51]. Modeling the SP–receptor interaction along the lines of our study on μ-opioid receptor [51] should help verify the general applicability of such a mechanism.

Acknowledgements

The authors thank Don Hughes and Brian Sayer of the McMaster NMR facility for valuable technical assistance in the NMR experiments. They also thank Dr Gary Shaw for his help with the initial NMR spectral measurements at the University of Western Ontario. This work was supported by a grant from the Medical Research Council of Canada.

REFERENCES

1. Regoli D, Boudon A, Fouchere J-L. Receptors and antagonists for substance P and related peptides. *Pharmacol. Rev*. 1994; **46**: 551–599.
2. Nicoll RA, Schenker C, Leeman SE. Substance P as a transmitter candidate. *Annu. Rev. Neurosci*. 1980; **3**: 227–268.
3. Schwyzer R. Peptide–membrane interactions and a new principle in quantitative structure–activity relationships. *Biopolymers* 1991; **31**: 785–792.
4. Stavropoulos G, Karagiannis K, Cordopatis P, Halle D, Gilon C, Bar-Akiva G, Selinger Z, Chorev M. Synthesis and biological activity of substance P *C*-terminal hexapeptide and heptapeptide analogues. *Int. J. Peptide Res*. 1991; **37**: 180–184.
5. Iwamoto I, Yamazaki H, Nakagawa N, Kimura A, Tomioka H, Yoshida S. Differential effects of two *C*-terminal peptides of substance P on human neutrophils. *Neuropeptides* 1990; **16**: 103–107.
6. Ohkubo H, Nakanishi S. Molecular characterization of the three tachykinin receptors. *Ann. New York Acad. Sci*. 1991; **632**: 53–62.
7. Quartara L, Maggi CA. The tachykinin NK1 receptor. Part II. Distribution and pathophysiological roles. *Neuropeptides* 1995; **32**: 1–49.
8. Rolka K, Erne D, Schwyzer R. Membrane structure of substance P: II. Secondary structure of substance P, [9-Leucine] substance P, and shorter segments in 2,2,2-trifluoroethanol, methanol, and liposomes studies by circular dichroism. *Helv. Chim. Acta*. 1986; **69**: 1798–1806.
9. Chassaing G, Convert O, Lavielle S. Preferential conformation of substance P in solution. *Euro. J. Biochem*. 1986; **154**: 77–85.
10. Sumner SCJ, Gallagher KS, Davis DG, Covell RL, Jernigan RL, Ferretti FA. Conformational analysis of the tachykinins in solution: substance P and physalaemin. *J. Biomol. Struct. Dyn*. 1990; **8**: 687–707.
11. Williams RW, Weaver JL. Secondary structure of substance P bound to liposomes in organic solvents and in solution from Raman and CD spectroscopy. *J. Biol. Chem*. 1990; **265**: 2505–2513.
12. Convert O, Duplaa H, Lavielle S, Chassaing G. Influence of the replacement of amino acid by its D-enantiomer in the sequence of substance P. 2. Conformational analysis by NMR and energy calculations. *Neuropeptides* 1991; **19**: 259–270.
13. Teleman O, von der Lieth C-W. Molecular dynamics simulation provides a possible structure for substance P-like peptides in aqueous solution. *Biopolymers* 1990; **30**: 13–23.
14. Schwyzer R. 100 years of lock-and-key concept: are peptides shaped and guided to their receptors by the target cell membrane? *Biopolymers* 1995; **37**: 5–16.
15. Schwyzer R. Membrane-assisted molecular mechanism of neurokinin receptor subtype selection. *EMBO J*. 1989; **6**: 2255–2259.
16. Pitner TP, Urry DW. Proton magnetic resonance studies in trifluoroethanol. Solvent mixtures as a means of delineating peptide protons. *J. Am. Chem. Soc*. 1972; **94**: 1399–1400.
17. Ananthanarayanan VS, Orlicky S. Interaction of substance P and its *N*- and *C*-terminal fragments with Ca^{2+}: implications for hormone action. *Biopolymers* 1992; **32**: 1765–1773.
18. Sergent DF, Bean JW, Schwyzer R. Reversible binding of substance P to artificial lipid membranes studied by capacitance minimization techniques. *Biophys. Chem*. 1989; **34**: 103–114.
19. Woolley GA, Deber CM. Peptides in membranes. Lipid-induced secondary structure in substance P. *Biopolymers* 1986; **26**: 109–121.
20. Duplaa H, Convert O, Sautereau AM, Tocanne JF, Chassaing G. Binding of substance P to monolayers and vesicles made of phosphatidylcholine and/or phosphatidylserine. *Biochem. Biophys. Acta* 1992; **1107**: 12–22.
21. Choo L-P, Jackson M, Mantsch HH. Conformation and self-association of the peptide hormone substance P: Fourier transform infrared spectroscopic study. *Biochem. J*. 1994; **301**: 667–670.

22. Young JK, Anklin C, Hicks RP. NMR and molecular modeling investigations of the neuropeptide substance P in the presence of 15 mM sodium dodecyl sulfate micelles. *Biopolymers* 1994; **34**: 1449–1462.
23. Keire DA, Fletcher TG. The conformation of susbtance P in lipid environments. *Biophys. J.* 1996; **70**: 1716–1727.
24. Cowsik SM, Lucke C, Ruterjans H. Lipid-induced conformation of substance P. *J. Biomol. Struct. Dyn.* 1997; **15**: 27–36.
25. Keire DA, Kobayashi M. The conformation and dynamics of substance P in lipid environment. *Protein Sci* 1998; **7**: 2438–2450.
26. Ananthanarayanan VS. Peptide hormones, neurotransmitters, and drugs as Ca^{2+} ionophores: implications for signal transduction. *Biochem. Cell Biol.* 1991; **69**: 93–95.
27. Pernow B. Substance P. *Pharmacol. Rev.* 1983; **35**: 85–141.
28. Fournier A, Couture R, Magnan J, Gendreau M, Regoli D, St-Pierre S. Synthesis of peptides by the solid-phase method. V. Substance P and analogs. *Can. J. Biochem.* 1980; **58**: 272–280.
29. Bax A, Davis DG. MLEV-17-based two-dimensional homonuclear magnetization transfer spectroscopy. *J. Magn. Reson.* 1985; **65**: 355–360.
30. Kumar A, Ernst RR, Wüthrich KA. A two-dimensional nuclear Overhauser enhancement (2D NOE) experiment for the elucidation of complete proton–proton cross-relaxation networks in biological macromolecules. *Biochem. Biophys. Res. Commun.* 1980; **95**: 1–6.
31. Wüthrich K. *NMR of Proteins and Nucleic Acids*. Wiley: New York, 1986; 117–174.
32. Bax A, Davis DG. Practical aspects of two-dimensional transverse NOE spectroscopy. *J. Magn. Reson.* 1985; **63**: 207–213.
33. Nemethy G, Pottle MS, Scheraga HA. Energy parameters in polypeptides. 9. Updating of geometrical parameters, nonbonded interactions and hydrogen bond interactions for the naturally occurring amino acids. *J. Phys. Chem.* 1983; **87**: 1883–1887.
34. Zhorov BS, Ananthanarayanan VS. Structural model of a synthetic Ca^{2+} channel with bound Ca^{2+} ions and dihydropyridine ligand. *Biophys. J.* 1983; **354**: 22–37.
35. Li Z, Scheraga HA. Monte Carlo minimization approach to the multiple minimum problem in protein folding. *Proc. Natl. Acad. Sci. USA* 1987; **84**: 6611–6615.
36. Zhorov BS. Vector method for calculating derivatives of energy of atom–atom interactions of complex molecules according to generalized coordinates. *J. Struct. Chem.* 1981; **22**: 4–8.
37. Zimmerman SS, Pottle MS, Nemethy G, Scheraga HA. Conformational analysis of the 20 naturally occurring amino acid residues using ECEPP. *Macromolecules* 1977; **10**: 1–9.
38. Brooks CL, Pettitt BM, Karplus M. Structural and energetic effects of truncting long ranged interactions in ionic polar fluids. *J. Chem. Phys.* 1985; **83**: 5987–5908.
39. Ananthanarayanan VS, Belciug M-P, Zhorov BS. Interaction of oxytocin with Ca^{2+}: II. Proton magnetic resonance and molecular modeling studies of conformations of the hormone and its Ca^{2+} complex. *Biopolymers* 1997; **40**: 445–464.
40. Rose GD, Geirasch LM, Smith JA. Turns in peptides and proteins. *Adv. Protein Chem.* 1985; **37**: 1–109.
41. Wüthrich K, Billeter M, Braun W. Polypeptide secondary structure determination by nuclear magnetic resonance observation of short proton–proton distances. *J. Mol. Biol.* 1984; **180**: 715–740.
42. Wishart DS, Sykes BD, Richards FM. Relationship between nuclear magnetic resonance chemical shift and protein secondary structure. *J. Mol. Biol.* 1991; **222**: 311–333.
43. Ananthanarayanan VS, Salehian O, Brimble KS. Interaction of gonadotropin releasing hormone and its analogs with Ca^{2+} in a nonpolar milieu. Correlation with biopotencies. *J. Peptide Res.* 1998; **52**: 185–194.
44. Regoli D, Dion S, Rhaleb N-E, Rouissi N, Tousignant C, Jukic D, D'Orleans-Juste P, Drapeau G. Selective agonists for receptors of substance P and related neurokinins. *Biopolymers* 1989; **28**: 81–90.
45. Wang J-X, Dipasquale AJ, Bray AM, Maeji NJ, Spellmeyer C, Geyson HM. Systematic study of substance P analogs II. Rapid screening of 512 substance P stereoisomers for binding to NK1 receptor. *Int. J. Peptide Protein Res.* 1989; **42**: 392–399.
46. Norinder U, Rivera C, Unden A. A quantitative structure–activity relationship study of substance P-related peptides. A multivariate approach using PLS and variable selection. *Int. J. Peptide Protein Res.* 1997; **49**: 155–162.
47. Saulitis J, Mierke DF, Byk G, Gilon C, Kessler H. Conformation of cyclic analogues of substance P: NMR and molecular dynamics in dimethyl sulfoxide. *J. Am. Chem. Soc.* 1992; **114**: 4818–4827.
48. Grdadolnik SG, Mierke DF, Byk G, Zeltser I, Gilon C, Kessler H. Comparison of the conformation of active and nonactive backbone cyclic analogs of substance P as a tool to elucidate features of the bioactive conformation: NMR and molecular dynamics in DMSO and water. *J. Med. Chem.* 1994; **37**: 2145–2152.
49. Byk G, Halle D, Zeltser I, Bitan G, Selinger Z, Gilon C. Synthesis and biological activity of NK-l selective, *N*-backbone cyclic analogs of the C-terminal hexapeptide of substance P. *J. Med. Chem.* 1996; **39**: 3174–3178.

50. Bikker JA, Trumpp-Kallmeyer S, Humblet C. G-protein-coupled receptors: models, mutagenesis and drug design. *J. Med. Chem.* 1998; **41**: 2911–2927.

51. Zhorov BS, Ananthanarayanan VS. Signal transduction within G-protein-coupled receptors via an ionic tunnel: a hypothesis. *J. Biomol. Struct. Dyn.* 1998; **15**: 631–637.